UNIVERSITÀ
DI PAVIA

PhD IN BIOMEDICAL SCIENCES

DEPARTMENT OF BRAIN AND BEHAVIORAL SCIENCES

UNIT OF NEUROPHYSIOLOGY

PHARMACOLOGICAL AND MOLECULAR BIOMARKERS IN PHARMACORESISTANT EPILEPSY

PhD Tutor: Prof. Emilio Perucca

PhD Co-Tutor: Dr. Valentina Franco

PhD Supervisor: Prof. Meir Bialer

PhD Supervisor: Prof. Emilio Russo

PhD dissertation of
Dr. Katia Baruffi

A.Y. 2018/19

TABLE OF CONTENTS

PHARMACOLOGICAL AND MOLECULAR BIOMARKERS IN PHARMACORESISTANT EPILEPSY

ACKNOWLEDGMENTS

I wish to express my sincere gratitude to my tutor, Professor Emilio Perucca, for his support and stimulating criticism throughout this work and for giving me the opportunity to spend three years in his research team, and my supervisor Dr. Valentina Franco for her unconditional encouragement and timely supervision throughout my work.

I also thank Dr. Cristina Cereda, Director of Genomic and post-Genomic Center at the IRCCS C. Mondino National Neurological Institute and her collaborators (Dr. Stella Gagliardi, Dr. Orietta Pansarasa and Dr. Daisy Sproviero) for their support and supervision during the conduction and interpretation of studies on miRNAs profiles, and for giving me access to the laboratory instrumentation required for these studies. My thanks are also due to Dr. Carlo Andrea Galimberti and Dr. Elena Tartara for providing the plasma samples from the patients with epilepsy included in these studies.

Dr. Fabio Blandini, Scientific Director of IRCCS C. Mondino National Neurological Institute, is gratefully acknowledged for providing the financial support required to conduct the studies on miRNAs profiles in extracellular vesicles.

My gratitude is also expressed to Dr. Cinzia Fattore, Mr. Roberto Marchiselli, and all members of the Unit of Clinical Pharmacology and Experimental Therapeutics of the Department of Internal Medicine and Therapeutics of the University of Pavia, for their help and friendship throughout this work. Ms. Elena Giovannetti is gratefully acknowledged for her excellent secretarial assistance.

Finally, I also wish to thank my parents and my sister for their love, and all other my colleagues and friends for their support and understanding.

SYNOPSIS

About one third of patients with epilepsy are pharmacoresistant and suffer from poor quality of life, seizure-related accidents and comorbidities, increased risk of death and disabling psychosocial consequences. Clinical outcomes for patients unresponsive to current pharmacological tools could be improved by characterization and development of biomarkers that could assist physicians in either (i) optimizing response to treatment with available antiepileptic drugs or (ii) identifying early those patients who are pharmacoresistant and could benefit from earlier referral to alternative therapies such as epilepsy surgery or neurostimulation. The work described in the present thesis addresses needs related to research on these two types of biomarkers.

The first part of the research relates to pharmacokinetic biomarkers aimed at optimizing response to pharmacological treatment. Specifically, plasma concentrations of antiepileptic drugs have been shown to provide valuable indicators of pharmacological response, although their usefulness has not yet been clearly established for some second-generation drugs, partly due to lack of availability of assay methods easily applicable to therapeutic drug monitoring in the routine setting. In the present research, the latter deficiency was addressed by developing and validating two assay techniques for the determination of retigabine, known also as ezogabine, and perampanel in body fluids. For retigabine, an HPLC-UV method suitable for therapeutic drug monitoring was developed which permits sensitive quantitation of the drug in human plasma. The method uses a simple solid-phase extraction for sample preparation and injection of the extract into the HPLC system. Chromatographic separation is achieved on a C18 Chromolith column connected to an ultraviolet detector set at 240 nm using. As mobile phase a mixture of water/acetonitrile/methanol (72:18:10, v/v/v) mixed with 0.1% of 85% phosphoric acid was used. Separation was carried out at 50°C with isocratic elution at a flow rate of 1.5 mL/min. Calibration curves were linear in the validated concentration range (25–2000 ng/mL). The assay is characterized by high precision (intra- and inter-day coefficients of variation ≤12.6%) and high accuracy (99.7%–108.7%) and can be conveniently applied to the investigation of concentration–response relationships in patients taking therapeutic doses of the drug. Although therapeutic drug monitoring of antiepileptic drugs is usually based on their determination in plasma samples, alternative matrices, such as dried plasma spots, may offer advantages in some settings. For this reason, a bioanalytical method for the quantitation of

perampanel in dried plasma spots was developed and validated. For sample preparation, two hundred microliters of plasma were distributed on a glass paper filter and dried. After addition of the internal standard promethazine, the analytes were extracted with methanol, dried at room temperature and reconstituted. Chromatographic separation of analytes was performed by using 2 C18 Chromolith columns connected to an ultraviolet detector set at 320 nm. As mobile phase, a mixture of water/acetonitrile (60:40, vol/vol) containing 0.1% of 85% phosphoric acid was used. Separation was carried out at 50°C with isocratic elution at a flow rate of 1.5 mL/min. Calibration curves were linear over the 25–1000 ng/mL concentration range. Intraday and interday precision (coefficients of variation) ranged from 2.8% to 8.6%, whereas intraday and interday accuracy were in the range of 99.2%–111.4%. Stability of the analyte in dried plasma spots was confirmed under different storage conditions. Perampanel concentrations assessed in dried plasma spot samples obtained from patients receiving therapeutic doses were comparable to those measured in plasma samples.

The second part of the research described in the present thesis relates to the investigation of microRNA (miRNA) profiles in plasma-derived extracellular vesicles as potential epigenetic biomarkers for early differentiation between patients resistant to antiepileptic drugs and patients responsive to these drugs. Additionally, miRNA expression profiles were also assessed in healthy controls in order to ascertain potential differences related to the disease itself rather than drug responsiveness. By applying a cross-sectional non-interventional open-label study design, miRNAs profiles in extracellular vesicles (exosomes and microvesicles) isolated from plasma were compared among three groups of individuals: 20 patients with drug-resistant focal epilepsy, 20 patients with drug-responsive focal epilepsy and 20 healthy control subjects. Microvesicle and exosome pellets were obtained with different centrifugation steps (20,000xg for microvesicle pellets and from the remaining supernatant 100,000xg to obtain exosome pellets). Extracellular purity, concentration and size distribution in each sample were ascertained by applying a combination of techniques (Western blot analysis, nanoparticle tracking analysis and transmission electron microscopy). Total RNA was extracted by exosome and microvesicle pellets. The RNA samples were used to produce cDNA libraries using the Small RNA-Seq Library Prep kit, and the libraries were sequenced on Next Generation Sequencing (NGS) platforms. The sequencing step was performed with NGS technologies using Illumina Genome Analyzer and the NextSeq 500/550 High Output v2.5 Illumina kit (150 cycles). RNA processing was carried out using Illumina NextSeq 500 Sequencing. Differential

expression analysis for miRNAs was performed with the R package DESeq2. MiRNAs with |log2(disease sample/healthy control)| ≥ 1 and a FDR ≤ 0.1 were considered differentially expressed. The potential involvement of identified miRNAs in epilepsy-relevant pathways (predicted target genes and predicted pathways) was investigated by using the miRWalk 3.0 database. A second search was conducted using the Kyoto Encyclopedia of Genes and Genomes (KEGG) database. Statistical analysis of the results did not identify significant differences across groups in extracellular vesicle size or count. A number of miRNAs were found to be differentially expressed in exosomes and microvesicles.

In exosomes, miR-145-5p and miR-3128 were significantly up-regulated and down-regulated, respectively, in patients with epilepsy compared with healthy controls. Five miRNAs were found to be de-regulated in exosomes isolated from pharmacoresistant patients compared with healthy controls. Specifically, miR-145-5p was up-regulated, whereas miR-3128, miR-3150a-3p, miR-3925-5p, and miR-6772-5p were down-regulated in pharmacoresistant patients. In microvesicles, three miRNAs were found to be de-regulated in patients with epilepsy compared with healthy controls: specifically, miR-183-5p was up-regulated, whereas miR-190a-5p, miR-93-3p were down-regulated. Four miRNAs were found to be de-regulated in microvesicles obtained from pharmacoresistant patients compared with healthy controls: these included two up-regulated miRNAs (miR-183-5p, miR-541-3p) and two down-regulated miRNAs (miR-26a-2-3p, miR-190a-5p). These findings, which require confirmation in a larger sample size, may provide valuable clues for a better understanding of processes involved in epileptogenesis as well as mechanisms implicated in pharmacoresistance.

LIST OF ABBREVIATIONS

ABCC1	ATP binding cassette subfamily C member 1
ABCC5	ATP binding cassette subfamily C member 5
AED	Antiepileptic drug
AMPA	α-amino-3-hydroxy-5-methyl-4-isoxazolepropionic acid
AMT PET	Alpha-methyl-tryptophan positron emission tomography
ANOVA	Analysis of variance
ARF6	ADP ribosylation factor 6
BCA	Bicinchoninic acid
BET	Bromodomain and extra-terminal
CBZ	Carbamazepine
cDNA	Coding DNA
CI	Confidence interval
CLB	Clobazam
CLN8	Ceroid-lipofuscinosis, neuronal 8
CNS	Central nervous system
CT	Computerized tomography
CV	Coefficients of variation
CYP2C19	Cytochrome P450 family 2 subfamily C member 19
ddATP	Dideoxyadenosine 5’-triphosphate
ddCTP	Dideoxycytidine 5'-triphosphate
ddGTP	Dideoxyguanidine 5'-triphosphate
ddNTP	Dideoxynucleoside Triphosphate
ddTTP	Dideoxythymidine 5'-triphosphate
DNA	Deoxyribonucleic acid
DPS	Dried spot plasma
DSSD	Dried sample spot device
ECG	Electrocardiogram
EEG	Electroencephalogram
EGFR	Epidermal growth factor receptor
F	Female
FAM3C	Family with sequence similarity 3 member C
FAQ	Frequently asked question
FDA	Food and Drug Administration
fMRI	Functional magnetic resonance imaging
GABA-A	γ-aminobutyric acid A
GABRG2	Gamma-aminobutyric acid type A receptor gamma2
GRIN2A	Glutamate ionotropic receptor NMDA type subunit 2A
HFO	High-frequency oscillation
HIV	Human immunodeficiency virus
HPLC-UV	High performance liquid chromatography-UV detection
ILAE	International League Against Epilepsy
IQR	Interquartile range
IS	Internal standard
ISEV	International Society for Extracellular Vesicles
JAK	Janus kinase

KCNMB4	Potassium calcium-activated channel subfamily M regulatory beta subunit 4
KCNQ2	Potassium voltage-gated channel subfamily Q member 2
KCTD7	Potassium channel tetramerization domain containing 7
KEGG	Kyoto Encyclopedia of Genes and Genomes
L2HGDH	L-2-hydroxyglutarate dehydrogenase
LCM	Lacosamide
LEV	Levetiracetam
LoA	Limits of agreement
LOD	Limit of detection
LOQ	Limit of quantification
LTG	Lamotrigine
M	Male
MDM2	Mouse double minute 2
MDR1	Multidrug-resistance-1
MEG	Magnetoencephalography
miRNA	microRNA
MRI	Magnetic resonance imaging
MRP	Multidrug resistance protein
MRS	Magnetic resonance spectroscopy
mTLE-HS	Mesial temporal lobe epilepsy with hippocampal sclerosis
NGS	Next generation sequencing
NTA	Nanoparticle tracking analysis
OXC	Oxcarbazepine
PB	Phenobarbital
PBS	Phosphate-buffered saline
PCA	Principal component analysis
PCR	Polymerase Chain Reaction
PER	Perampanel
PET	Positron emission tomography
PGB	Pregabalin
P-gp	P-glycoprotein
PHT	Phenytoin
PRM	Primidone
PVDF	Polyvinylidene fluoride
QC	Quality control
RCN2	Reticulocalbin 2
RE1	Repressor element 1
REST/NRSF	RE1-silencing transcription factor/neuron-restrictive silencer factor
RIPA	Radio-Immunoprecipitation Assay
RNA	Ribonucleic acid
RTN4	Reticulon 4
SCN1A	Sodium voltage-gated channel alpha subunit 1
SD	Standard deviation
SDS	Sodium dodecyl sulfate
SLC6A8	Solute carrier family 6 member 8

SNP	Single nucleotide polymorphism
SPECT	Single photon emission computed tomography
SSTR2	Somatostatin receptor 2
STAT	Signal inducers and activators of transcription
TBS-T	Tris-buffered saline - Tween
TDM	Therapeutic drug monitoring
TMS	Transcranial magnetic stimulation
TPM	Topiramate
VPA	Valproic acid
WASL	WASP [Wiskott-Aldrich Syndrome protein] like actin nucleation promoting factor
ZNS	Zonisamide

1. INTRODUCTION

1.1 Epilepsy and seizures

Epilepsy is the most prevalent chronic brain disorder and is defined conceptually as an enduring predisposition to generate epileptic seizures with all the neurobiological, cognitive, psychological, and social consequences of this condition (Fisher et al, 2005). According to the International League against Epilepsy (ILAE), epilepsy can be defined operationally as any of the following conditions: (1) at least two unprovoked (or reflex) seizures occurring >24 h apart; (2) one unprovoked (or reflex) seizure and a probability of further seizures similar to the general recurrence risk (at least 60%) after two unprovoked seizures, occurring over the next 10 years; (3) diagnosis of an epilepsy syndrome (Fisher et al, 2014). Epilepsy may not last forever. According to the ILAE definition, epilepsy should be considered to have resolved when: i) a subject who received a diagnosis of epilepsy has been seizure-free for the last 10 years, 5 of which without pharmacological therapy; (ii) the diagnosis of an age-dependent epilepsy syndrome becomes incompatible with the age of the individual (Fisher et al, 2014).

An epileptic seizure can be defined as an acute and transient manifestation of symptoms/signs due to abnormal, rhythmic and synchronous firing of populations of neurons in the brain (McNamara, 1999). After a first event, the probability of having a second seizure can be predicted based on a number of factors such as the seizure type, the epilepsy syndrome, the underlying etiology (if known), the presence/absence of interictal electroencephalogram (EEG) abnormalities, and other patient-related factors such as age, presence of associated neurological abnormalities, and presence of comorbid conditions.

With a prevalence estimated at 0.7-0.9%, epilepsy affects about 65 million people worldwide (Moshé et al. 2015), and it is associated with increased morbidity and mortality (Kwon et al., 2010). The prevalence of active epilepsy is higher in low- and middle-low income countries (10 per 1000 population) than in high-income countries (5-8 per 1000 population). This difference is explained by differences in access to health care and in exposure to epileptogenic insults such as central nervous system (CNS) infections and perinatal damage (Moshé et al., 2015). Likewise, the annual incidence of epilepsy is related to socio-economic conditions and varies from 81.7 per 100,000 population (Interquartile Range [IQR] 28.0-239.5) in low- and middle-income countries to 45.0 per 100,000 population (IQR 30.3-66.7) in high-income countries (Ngugi et al. 2011). Epilepsy is often associated with social stigma, various comorbidities (particularly psychiatric comorbidities) and high direct medical costs.

The first ILAE classifications of epileptic seizures and epilepsies were published about 50 years ago (Gastaut, 1969; Gastaut, 1970), and updated in 1981 and 1989 for seizures (ILAE, 1981) and epilepsies (ILAE, 1989) respectively. The 1989 ILAE classification differentiated epilepsies into three categories: (i) idiopathic epilepsies (epilepsies not associated with a structural lesion, neurologic abnormalities or cognitive impairment, and considered to be genetic in origin); (ii) symptomatic epilepsies (seizures as a consequence of a brain lesion or insult) and (iii) cryptogenic epilepsies (epilepsies with unknown but presumed symptomatic aetiology).

The 1989 ILAE classification of epilepsy and seizures was replaced in 2017 by a new framework which was developed to include the major scientific advances that have taken place during the last three decades (Figure 1).

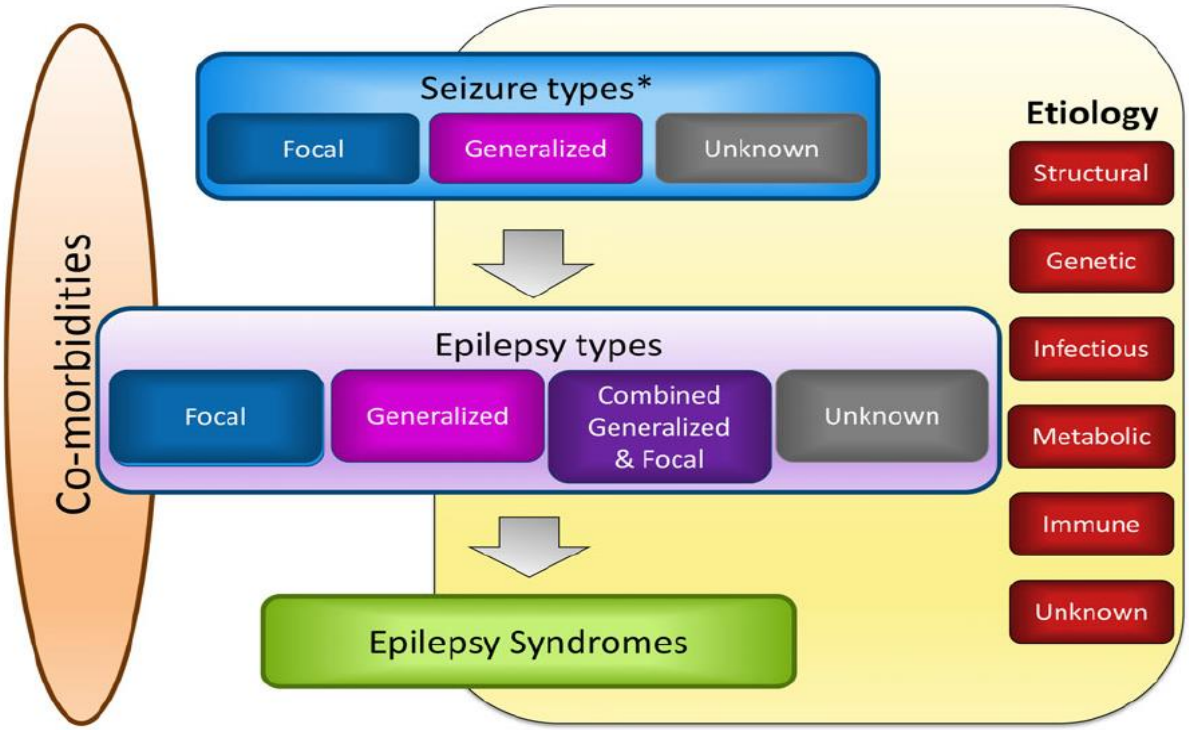

Figure 1. The current ILAE classification of seizures and epilepsies (Scheffer et al, 2017).

The latest classification is organized along three levels, starting with type of seizures, classified according to the 2017 ILAE Classification (Scheffer et al, 2017). After the seizure type

diagnosis, the next level is epilepsy type diagnosis (focal epilepsy, generalized epilepsy, combined generalized and focal epilepsy, and unknown epilepsy). The next step is to define the epilepsy syndrome, when possible. In addition, the new classification includes at each stage etiology, divided into six subgroups which are relevant for their potential therapeutic consequences. A comorbidity axis is also included.

Seizures are categorized as focal-, generalized- or unknown-onset. Focal seizures are those that originate within networks limited to one hemisphere (including, at times, subcortical structures) and may be discretely localized or more widely distributed. For each focal seizure type, ictal onset is consistent from one seizure to another, with preferential propagation patterns that can involve the contralateral hemisphere. By contrast, generalized seizures begin at some point within rapidly engaging bilaterally distributed networks; they can include cortical and subcortical structures, but do not necessarily include the entire cortex. Although individual generalized seizure onsets can appear localized, the location and lateralization are not consistent from one seizure to another. Generalized seizures can be asymmetric. According to current ILAE classification, seizures are also classified based on the presence/absence of awareness, and their main semiological features, as shown in Figure 2.

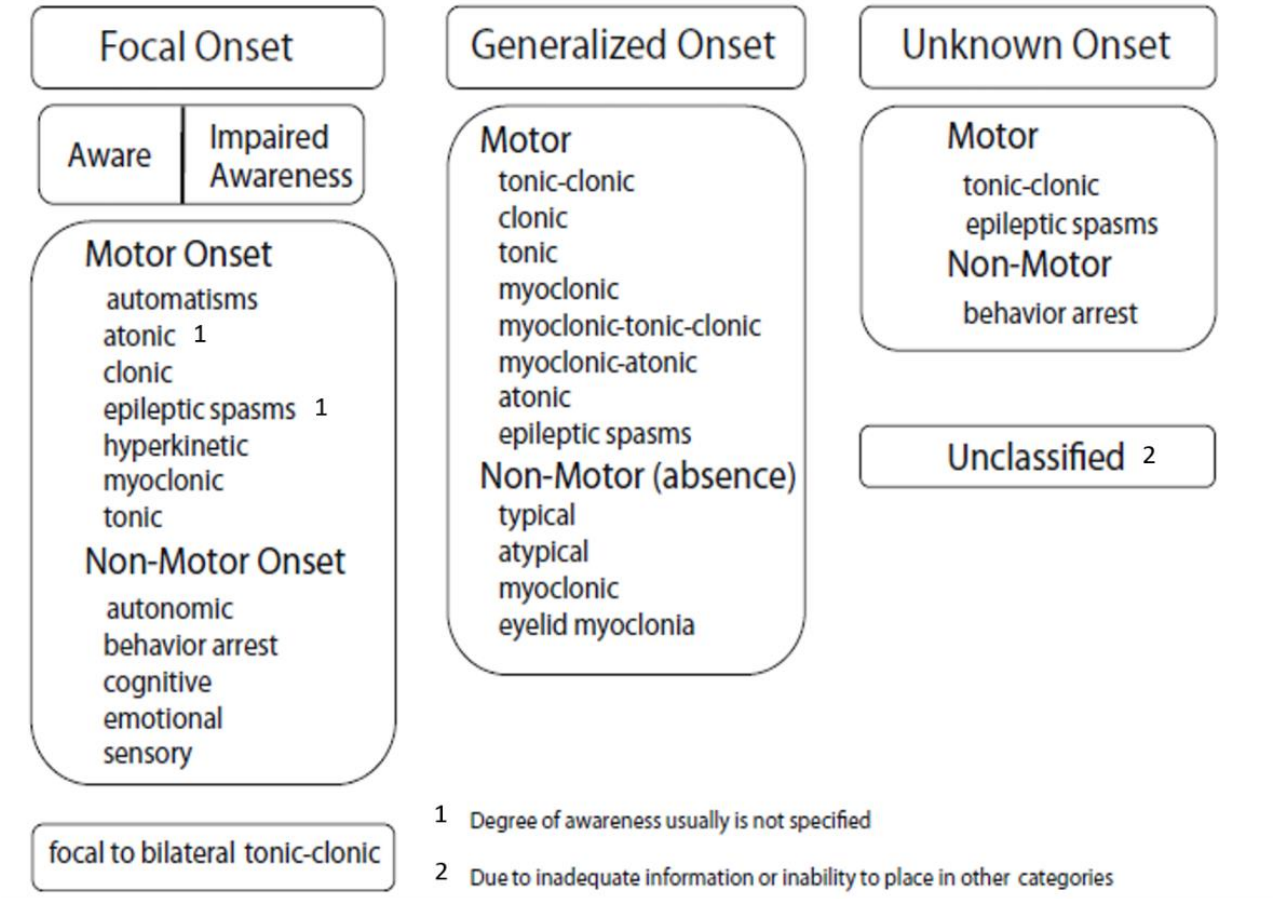

Figure 2. The current ILAE classification of seizures types (modified from Fisher et al., 2017).

1.2 Diagnostic issues

An accurate clinical diagnosis of epilepsy is essential for correct management and is usually based on a precise description of seizure events and other factors such as age of seizure onset, neurological findings, family history, interictal EEG, neuroimaging evaluation and a 12-lead electrocardiogram (ECG) to exclude cardiac abnormalities. Some syndromes are easily identified, as in the case of self-limited childhood epilepsy with centrotemporal spikes, childhood or juvenile absence epilepsy and juvenile myoclonic epilepsy. When a specific structural cause is suspected, magnetic resonance imaging (MRI) can be helpful. Today, advanced imaging technologies can identify tiny epileptogenic lesions. Likewise, advances in genetics allow identification of epilepsy gene mutations which are pathogenic for many syndromes, particularly epileptic encephalopathies (Devinsky et al., 2018).

Despite improvement in diagnostic techniques, about 25% of patients are misdiagnosed, with consequent potentially inappropriate treatment (Ferrie, 2006). Misinterpretation of the EEG findings is a common cause of diagnostic errors.

1.3 Pharmacological treatment options

The treatment of epilepsy is aimed at achieving seizure freedom without adverse effects. Pharmacological treatment should be individualized depending on the patient's characteristics and the properties of the drugs (Perucca and Tomson 2011; Raspall-Chaure et al., 2008). Drug-related factors influencing the choice of medications include: (i) the efficacy of antiepileptic drugs (AEDs) on different types of seizures or syndromes; (ii) the tolerability and safety profile of the AEDs; (iii) the therapeutic index of the medications (the difference between efficacious and toxic doses); (iv) pharmacokinetic profile; (v) drug-drug interactions; (vi) approved indications, and contraindications; (vii) comorbidities; (viii) available formulations; (ix) cost and reimbursability. Patient-related factors to be considered for their impact on outcome include seizure/epilepsy type, age, gender, comorbidities, comedications and risk factors for adverse effects.

The general approach to epilepsy treatment is to use first a monotherapy, which is effective in approximately 50% of patients without causing relevant adverse effects. The advantages of using a single drug are a high efficacy, no drug interactions and better tolerability compared to polytherapy. In patients with persisting seizures after the first monotherapy, re-evaluation of the diagnosis and drug selection is crucial. Among non-responders to the first monotherapy, an additional 15-20% of patients achieve seizure remission with an alternative monotherapy. A polytherapy regimen is generally introduced after two or three inappropriate therapeutic regimens with a single drug have failed to control the seizures, even though only a relatively small number of patients unresponsive the two appropriately chosen AEDs will achieve seizure freedom on other treatments (Perucca and Tomson, 2011).

1.4 The challenge of drug resistant epilepsy

Pharmacoresistance in epilepsy was defined in 2010 by the ILAE as failure to achieve sustained seizure freedom after adequate trials of two tolerated and appropriately prescribed AED

schedules (as monotherapies or in combination) to produce sustained seizure freedom (Kwan et al., 2010). Pharmacoresistance occurs in approximately 20-30% of all patients with epilepsy (Regesta and Tanganelli, 1999). This condition is associated with an increased risk of death and disabling psychosocial consequences (Schmidt and Löscher, 2005) and for this reason represents one of the major challenges in epilepsy management. Not all types of epilepsy have the same proportion of pharmacoresistance, with some syndromes (e.g. epileptic encephalopaties) having a far worse response to treatment than others (e.g. juvenile myoclonic epilepsy).

Uncontrolled seizures and drug toxicity (often associated with polytherapy and high AED doses) are frequently associated with learning disability, intellectual impairment, psychiatric comorbidities, autonomy reduction, worsening of quality of life, and risk of seizure-related sudden death (Wirrell, 2013). Although drug-resistance usually is diagnosed early in the course of the disease, it can also occur after several years and be preceded by a prolonged seizure-free period. Certain etiologies and a high seizure frequency are predictors of poor response to treatment. In particular, pharmacoresistance often occurs in patients with epileptic encephalopathies, documented cortical dysplasia and hippocampal sclerosis (Rogawski, 2013; Wirrell, 2013). Seizures persistence leads to greater use of polytherapy, often resulting in increased side effects, a marked reduction in the quality of life, higher direct medical costs and increased mortality.

Several newer AEDs have been introduced in the last three decades for the management of drug resistant epilepsy. However, their impact on long-term outcome in these patients is overall modest (Perucca and Kwan, 2005). Available data from clinical trials indicate that about 5-10% of patients with refractory epilepsy can be made seizure free by newer AEDs (Perucca, 2002; Walker and Sander, 1997). In this context, a critical point to consider is that use of AEDs in clinical trials differs from clinical practice, and many epilepsy syndromes have never been investigated in well designed randomized trials (Perucca, 2002; Walker and Sander, 1997). Epilepsy surgery has the greatest chance of achieving seizure control in patients with pharmacoresistant epilepsy, but eligibility criteria for surgery (focal epilepsy with a clearly defined epileptogenic zone in a non-eloquent part of the brain) restrict the number of suitable candidates.

Extensive research is ongoing to elucidate the molecular basis of drug resistance and facilitate discovery of more effective AEDs. Mechanism-based approaches focus on anti-epileptogenic targets, multi-drug transporters reversal/inhibitors, drug target alterations, and drugs targeting neuroinflammatory pathways.

1.5 Addressing mechanisms responsible for therapeutic failure

1.5.1 Pharmacokinetic variability

All the drugs used to treat epilepsy show extensive pharmacokinetic variability (Patsalos et al., 2018). This implies that there is a large variability in serum AED concentrations among patients receiving the same dose. This, in turns, results in a wide variability in the concentration of the same drugs at their site of action in the brain and, consequently, marked inter-individual differences in clinical response (Patsalos et al., 2018). Failure to achieve adequate serum AED concentrations is an important cause of treatment failure, and contributes in a major way to the so called-phenomenon of pseudo-pharmacoresistance.

To ascertain mechanisms involved in suboptimal pharmacological responses and to provide guidance to dosage adjustment, therapeutic drug monitoring (TDM) may be applied. The monitoring of serum AED concentrations can be useful to (i) establish the individual serum/plasma concentration required to achieve seizure control with minimal adverse effects (the so-called "individual therapeutic concentration/range"); (ii) identify potential causes of therapeutic failure (poor compliance, poor drug absorption, fast metabolism, drug-drug interactions); (iii) differentiate manifestations of drug toxicity from symptoms of the underlying disease; (iv) optimize dosage in special populations showing altered pharmacokinetic properties, for example in children (where AED pharmacokinetics may change prominently over time from neonatal age to infancy, childhood and adolescence), during pregnancy and breastfeeding, and in the elderly, in whom pharmacokinetics may be affected by aging-related decline in renal and metabolic function, the impact of comorbidities on drug absorption and disposition, and interactions caused by concomitantly administered medications; (v) adjust dosage to compensate for the influence of concomitant therapies and related drug-drug interactions, particularly in drug resistant patients; (vi) identify potential pharmacokinetic changes related to use of different drug formulations or generic substitution (Patsalos et al., 2018). Two generations of AEDs are currently used in clinical management. The "first-

generation" includes carbamazepine, ethosuximide, phenobarbital, phenytoin, primidone, valproic acid and the benzodiazepines, which were introduced in the market prior to 1970. The "second generation" refers to drugs approved in Europe and/or in United States in the last 30 years and includes brivaracetam, cannabidiol, eslicarbazepine acetate, felbamate, gabapentin, lacosamide, lamotrigine, levetiracetam, oxcarbazepine, perampanel, pregabalin, retigabine, rufinamide, stiripentol, tiagabine, topiramate, vigabatrin, and zonisamide. Therapeutic monitoring of serum drug concentrations is best established for first-generation AEDs, but increasing evidence indicates that its application can also be valuable to optimize dosage of newer medications (Patsalos et al., 2018).

1.5.2 Pharmacodynamic variability

Each AED has one or more targets in the brain, such as voltage-dependent ion channels, neurotransmitter receptors or transporters, and enzymes or modulatory sites involved in neurotransmitters metabolism, uptake, and release. Alterations in the structure and/or function of these targets may reduce the efficacy of AEDs. In fact, the causes of drug resistance may be multifactorial and also include alterations in AED transporters across the blood-brain barrier, neural networks, and genetic variants (Löscher et al., 2013). Four different hypotheses, not mutually exclusive, have been proposed as potential mechanisms drug resistance: the network hypothesis, the target hypothesis, the transporters hypothesis, and the genetic hypothesis.

The network hypothesis is supported by the fact that recurrent seizures alter brain plasticity and induce network changes potentially causing drug-resistance. This condition is common in hippocampal sclerosis (Fang et al., 2011).

The target hypothesis implies that a reduced AED efficacy can be determined by an alteration in structure and/or function of its target site(s) in the brain. One example relates to AEDs that act at least in part as inhibitors of voltage-gated sodium channels (e.g. carbamazepine, oxcarbazepine, eslicarbazepine, lacosamide, lamotrigine, phenytoin, topiramate and zonisamide). In studies conducted in vitro in hippocampal neurons and dentate granule cells obtained from pharmacoresistant patients, sodium channels have been found to show a reduced use-dependent inhibition by carbamazepine (Remy et al., 2003; Vreugdenhil et al., 1998). An altered subunit types expression induced by seizures or by acquired causes, or a genetically induced alteration are possible mechanisms that could determine loss of sodium channel drug

sensitivity and induce drug-resistance. Another possible example is represented by changes in GABA-A receptors, that in pharmacoresistant patients may show altered subunit expression, altered distribution or altered shift from inhibitory to excitatory state resulting in pharmacological insensitivity (Cohen et al., 2003; Loup et al., 2000; Volk et al., 2006). The target hypothesis, however, does not explain why most patients are resistant to several AEDs with different mechanisms of action. Therefore, it must be assumed that in these patients other factors probably contribute to drug resistance.

The drug transporter hypothesis associates drug resistance with overexpression of multidrug efflux transporters. These transporters affect drug absorption, disposition and elimination and have an important role in causing failure to respond to certain medications (Schinkel and Jonker, 2003). P-glycoprotein (P-gp), in particular, is a drug efflux transporter, member of the multidrug resistance protein (MRP) family, which is encoded by the human multidrug-resistance-1 (MDR1; ABCB1) gene. P-gp is expressed in endothelial cells, in particular in the blood brain barrier, and in astrocytes, neurons, and tissues with excretory function (small intestine, liver and kidney), with a broad substrate specificity extending to many structurally divergent drugs (Fromm, 2004). Some studies have associated P-gp overexpression to a limited access of several AEDs to the brain parenchyma, resulting in loss of their seizure-suppressing effects (Kwan and Brodie, 2005; Schmidt and Löscher, 2005; Tishler et al., 1995).

Genetic variations can affect any of the above mechanisms. For example, single nucleotide polymorphisms (SNPs) can affect both drug targets and drug transporters provoking alterations in AED responsiveness. Pharmacogenetic studies focused on *SCN1A*, the gene encoding for the α-subunit of the voltage-gated sodium channel in the CNS, variations of which associated different SNPs can cause an altered response to phenytoin, carbamazepine, lamotrigine and oxcarbazepine (Depondt and Shorvon, 2006). A common SNP within exon 26 of MDR1 gene was initially associated to overexpression of P-gp and pharmacoresistant epilepsy (Siddiqui et al., 2003) but subsequent studies have not confirmed this finding (Basic et al. 2008).

1.5.3 Role of biomarkers in addressing mechanisms of treatment failure

Pharmacoresistant epilepsy represents a significant burden not only for patients and their families, but also for health care systems. Despite introduction of several new AEDs in the last three decades, the percentage of patients with pharmacoresistant epilepsy has not been reduced

substantially since the late 60s, and development of innovative therapies is stagnating. Management of epilepsy is still based on a "trial-and-error" approach because we lack reliable tools, such as biomarkers, which could help us to (i) optimize treatment with existing AEDs, for example by facilitating optimization of dosage or identifying individuals more likely to respond to specific medications; (ii) identify mechanisms of drug resistance, and lead to rational design of more effective drugs acting on those mechanisms.

One area where extensive biomarker research is ongoing relates to epileptogenesis and ictogenesis. As stated eloquently by Engel et al (2013), "*biomarkers of epileptogenesis, the development of epilepsy, and ictogenesis, the propensity to generate spontaneous seizures, could (i) predict the development of an epilepsy condition, (ii) identify the presence and severity of tissue capable of generating spontaneous seizures, (iii) measure progression after the condition is established, (iv) be used to create animal models for more cost-effective screening of potential antiepileptogenic and antiseizure drugs and devices, and (v) reduce the cost of clinical trials of potential antiepileptogenic interventions by enriching the trial population with patients at high risk for developing epilepsy, and both antiepileptogenic and anti-seizure interventions by serving as a surrogate marker for spontaneous behavioural seizures*." The availability of such biomarkers would have important consequences for diagnosis and prognosis, and could potentially prevent the development of epilepsy by identifying patients at risk and making antiepileptogenic treatments available to them (Engel et al., 2013; Galanopoulou and Moshé, 2011).

High throughput methodologies applied to body fluids (blood, plasma, saliva, cerebral spinal fluid, urine, biopsy-derived tissues) are being applied to obtain massive information about thousands of biological molecules that may be differentially expressed in specific diseases, like epilepsy (Raoof et al., 2017). In this context, main areas of epilepsy 'big-data'-based biomarker research include genomics, metabolomics, lipidomics and proteomics (Loeb, 2010). The process that leads to the identification of a biomarker typically includes three phases: (i) discovery – strategy for the identification of candidates markers; (ii) validation – demonstration in animal models and in clinical studies that the biomarker meets its prerequisites, for example in predicting development of epilepsy or response to therapy, (iii) translation – the planning of experiments to apply the biomarker to interventions aimed at improving the efficiency of preventive, diagnostic or therapeutic processes. Danhof and colleagues (Danhof et al., 2005) classified biomarkers into 6 categories on the base of cascading types that relate treatment to

pathophysiology, in order to allow a prediction of drug effects in vivo: genotype or phenotype (type 0), drug concentration (type 1), target occupancy (type 2), target activation (type 3), physiological response (type 4), pathophysiological response (type 5) and clinical scale (type 6).

Biomarker are also recognized by regulators as valid tools applicable to preclinical and clinical drug development. In this context, biomarkers may be used as surrogate markers for specific pathophysiological process. A surrogate marker is defined by the Food and Drug Administration (FDA) as *"a laboratory measurement or physical sign that is used in therapeutic trials as a substitute for a clinically-meaningful endpoint that is a direct measure of how a patient feels, functions, or survives, and is expected to predict the effect of the therapy*" (Katz, 2004).

1.5.3.1 Pharmacokinetic biomarkers

As discussed above in the section 'Pharmacokinetic variability', serum AED concentrations can be used as biomarkers to guide individualization of dosage, to identify pharmacokinetic causes of treatment failure, to predict the probability of achieving therapeutic success, and to implement interventions to optimize clinical response. For these objectives to be achieved, a number of conditions need to be met: (i) a laboratory method has to be developed that permits monitoring of the concentration of the drug(s) of interest in serum or other body fluids with adequate accuracy, precision, sensitivity and specificity, as well as easy applicability to TDM in the clinical setting; (ii) information should be obtained on the pharmacokinetic characteristics of the drug(s) of interest, the relationship between its concentration in serum (or other body fluids) and dosage both within and between patients, as well as factors influencing such relationship; (iii) methodologically sound data should the obtained on the relationship between the concentration of the drug(s) of interest in serum or other body fluids and clinical response, both in terms of seizure control and appearance of adverse effects, as well as factors influencing such relationship; (iv) well designed studies should be conducted to validate the value of TDM in improving clinical outcomes in the population of interest. Part of the work described in the present thesis relates to the first in this sequence of activities.

1.5.3.2 Genetic and epigenetic biomarkers

The investigation of the mechanisms that lead to epileptogenesis is a crucial step in order to rationally develop new therapies. Epileptogenesis involves a complex change in CNS cell communication taking place along different steps, starting with an initial insult (stroke, traumatic insult, brain infection, presence of neurotoxins) and proceeding through sequential changes in signaling and consequent modifications in gene expression and epigenetic landscape. Altered gene expression can induce changes in ion channel activity, neurotransmitter receptor expression, and can provoke inflammation, axonal and dendritic plasticity, gliosis and neuronal cell death (Pitkanen and Lukasiuk, 2011). During the latent phase of epileptogenesis, many changes can occur in synaptic circuitry, seizure activity, and neurogenesis with or without clinical symptoms (Younus and Reddy, 2017). The resulting epigenetic profile is dependent on the cellular and extracellular environment. Epigenetic modifications significantly altered in the epileptic brain include DNA-methylation, micro-RNA-based transcriptional control, bromodomain reading activity, and other processes, summarized in Figure 3.

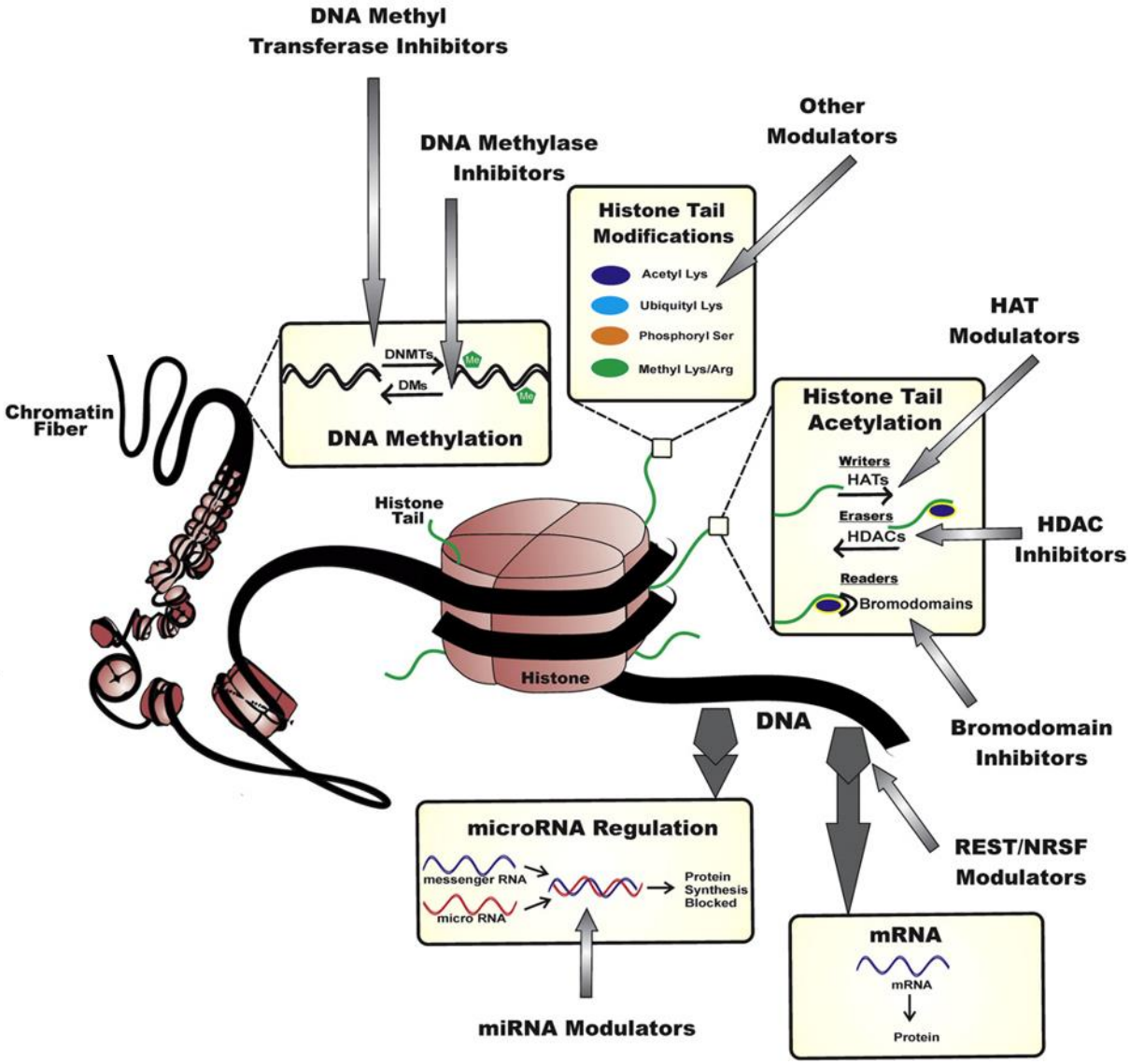

Figure 3. Representation of potential epigenetic mechanisms and related inhibitors in epilepsy (modified from Younus and Reddy, 2017).

In fact, chronic epilepsy can be characterized as a pathological state supported by an array of altered mechanisms such as DNA methylation, histone acetylation, miRNA expression, bromodomain and extra-terminal (BET) inhibition, and repressor element (RE)1-silencing transcription factor/neuron-restrictive silencer factor (REST/NRSF) (Pitkanen and Lukasiuk, 2011). Many of these processes are reversible, and therefore they are potential therapeutic targets. For example, histones, proteins that regulate the DNA over-structure, have many sites that can be post-translationally modified on the N-terminal tails with lysine ubiquitination,

acetylation and methylation, arginine methylation, and serine phosphorylation. The choice of therapeutic target may be influenced by the type of site-specific epigenetic modification.

Histone modifications have a particular role that can alter chromatin structure and influence changes to the overall epigenetic profile. For example, epileptogenesis may be triggered by induction of RE1-silencing transcription factor or by the activation of transcriptional pathways by Janus kinase (JAK)-signal inducers and activators of transcription (STAT). In animal models, hypomethylation of DNA occurs within 1 day of experimental status epilepticus (gene activation), while DNA hypermethylation has been reported in patients with temporal lobe epilepsy (Devinsky et al., 2018). DNA methyltransferase inhibitors can inhibit seizure onset, especially when administered in conjunction with agents that up-regulate adenosine and glycine, i.e. agents that provide methylation equilibrium. Acetylation is catalyzed by histone acetyltransferases that confer a less compact increasing transcriptional activity, while deacetylation is promoted by histone deacetylases that have an important role in the repression of gene transcription. Changes in histone acetyltransferase activity have been found to be involved in neurogenesis, memory formation, neuroplasticity, and synaptogenesis. For this reason, histone acetyltransferase is one of the targets being considered in the development of novel antiepileptogenic and antiseizure treatments. Seizure activity may be ameliorated when AEDs are administered with histone deacetylase inhibitors, such as valproic acid (Younus and Reddy, 2017).

During epileptogenesis, ion channel expression is altered by transcriptional and epigenetic mechanisms that modify gene expression. For example, alterations in transcription of calcium channel (such as Cav3.2 channels) promotes, when it is up-regulated, or attenuates, when it is inhibited, the onset of seizures. MicroRNAs (miRNAs) expression is also altered during epileptogenesis, probably because miRNAs target the signaling that controls brain development, dendritogenesis, synaptogenesis, neurotransmitter receptors, inflammation, and regulatory feedback on transcriptional regulators (e.g., DNA methyltransferase and histone deacetylases).

MiRNAs are a small fragment (19-24 nucleotide sequence) of non-coding RNA which are physiologically produced in cells and regulate gene expression by targeting multiple messenger RNAs (mRNAs). The monitoring of changes in miRNA levels in brain or in body fluids could potentially allow identification of early epileptogenesis onset and disease progression. As

detailed below, evaluation of miRNA as potential biomarkers of pharmacoresistance represents one of the aims of the work described in the present thesis.

1.5.3.3 Neurophysiological biomarkers

The interictal EEG spike is a well known biomarker of epileptic activity, and assessment of its presence/absence and localization is part of the routine diagnostic workup in epilepsy. High-frequency oscillations (HFOs), which are brief 80–00 Hz electrical events (divided into ripples (80–250 Hz) and fast ripples (> 250 Hz)) typically recorded by intracranial electrodes, have attracted considerable interest as biomarkers of epileptogenesis. Based on studies in rodent models, ripple frequency oscillations are considered to be physiological in the hippocampus whereas fast ripple frequency oscillations are considered to be pathological, indicating epileptogenic tissue. The distinction between physiological or pathological HFOs may not be always simple. Clinical studies using intracranial microelectrodes have demonstrated that HFOs can be reliable indicators in delineating the epileptogenic region and in defining the extent of tissue that needs to be removed by surgical intervention. HFOs increase immediately prior or at seizure onset and are confined to the same epileptogenic area during ictal and interictal periods while spikes are more widespread during seizures (Pitkanen et al., 2016).

A non-invasive tool used at times to assess cortical excitability is the transcranial magnetic stimulation (TMS). TMS combined with EEG allows investigating the reactivity (i.e. excitability and connectivity) of the cortex to a focal stimulation. Some studies suggest that late responses to magnetic pulses (registered 100-1000 msec after stimulus) may identify increased cortical excitability and connectivity in patients with focal epilepsy. Technical limitations (need for dedicated instrumentation, difficulties in controlling technical artifacts, long duration of the testing, and difficulties in processing and interpreting EEG responses) have confined application of TMS-EEG testing to research laboratories only (Sueri et al., 2018).

1.5.3.4 Imaging biomarkers

Several neuroimaging techniques are useful for diagnosis and assessment of patients with epilepsy. These include computerized tomography (CT), structural and functional magnetic resonance imaging (fMRI), MR spectroscopy (MRS), EEG combined with fMRI (EEG/fMRI),

positron emission tomography (PET), ictal and interictal Single Photon Emission Computed Tomography (SPECT), and magnetoencephalography (MEG) (Engel et al., 2013). MRI permits to identify common epileptogenic lesions, including some prenatal or perinatal cerebral injuries, malformations of cortical development, tumors, post-stroke or post-traumatic encephalomalacia, vascular anomalies and hippocampal sclerosis. This technique is more efficient than CT, that remains more widely available, faster and with fewer contraindications. Epilepsy-specific protocols and interpretation of MRI results by expert neuroradiologists permit efficient identification of epileptogenic lesions, inform prognosis, guide management, and are essential in presurgical evaluation when AEDs do not permit to achieve seizure control.

The functional interactions between brain regions that are not directly connected may be detected by fMRI. This technique highlights the differences in blood oxygen level-dependent contrast between target and control condition and reveals brain area/s that perform a particular activity (e.g. movement, memory, language, etc.). For example, studies that utilized fMRI predicted a more significant decline in verbal memory after resection when a stronger pre-resection activation lateralization to the dominant hemisphere (dominant frontal or dominant temporal region) was detected. In the last decade, EEG/fMRI has been applied to provide additional insights into the localization of the epileptogenic zone (Middlebrooks et al., 2017; Pitkanen et al., 2016). Recently, application of the MRI technique to assessment of patients with drug-resistant mesial temporal lobe epilepsy led to identify a significant reduction in fractional anisotropy in the white matter of the temporal lobes and a reduced cortical thickness of the corpus callosum, which were considered as potential biomarkers of pharmacoresistance (Pitkanen et al., 2016).

Among other imaging-related biomarkers, positron emission tomography with alpha-methyl-tryptophan (AMT PET) has allowed to demonstrate that in seizure patients with tuberous sclerosis and multiple tubers alpha-methyl-tryptophan concentrates in epileptogenic tuber(s), and that surgical removal of these tubers can result in seizure remission (Kumar et al., 2011).

Two recent proof-of-concept studies provided evidence that epileptogenesis after certain brain insults can be identified with acceptable sensitivity and specificity by using MRI-based techniques. In particular, Immonen et al. (2013) reported that seizure susceptibility at 12 months after traumatic brain injury was predicted by a combination of MRI measures evaluated within the first two post-injury months. Another study conducted by Choy et al. (2014) in a rat model

found that amygdala T2 values assessed two hours after experimental febrile status epilepticus identified reliably those animals in which the insult led to development of epilepsy.

1.6 Rationale for the research described in the present thesis

About one third of patients with epilepsy are pharmacoresistant and suffer from poor quality of life, seizure-related accidents and comorbidities, increased risk of death and disabling psychosocial consequences. Clinical outcomes for patients unresponsive to current pharmacological tools could be improved by characterization and development of biomarkers that could assist physicians in either (i) optimizing response to treatment with available AEDs or (ii) identifying early those patients who are pharmacoresistant and could benefit from earlier referral to alternative therapies such as epilepsy surgery or neurostimulation. Any biomarker that could allow early differentiation between AED responsive and pharmacoresistant patients could also provide clues into the mechanisms of drug resistance, and facilitate the rational design of novel drugs targeting such mechanisms. The work described in the present thesis addresses both of these unmet needs, by focusing on two issues: (i) pharmacokinetic biomarkers, through development of assay techniques for the determination of recently introduced AEDs in body fluids in order to permit exploration of the potential value of TDM as a tool to optimize clinical response to these agents; (ii) epigenetic biomarkers, with the aim of identifying a early predictors of pharmacoresistance and, potentially, providing a clue into the mechanisms underlying drug resistance.

1.6.1 Development of assay methods for the determination of recently introduced AEDs in body fluids

Among the AEDs introduced in the market in the last decade, two compounds stand out because of their mechanisms of action, which differ from the mechanisms of action of other available agents. These drugs are retigabine (ezogabine), an activator of potassium channels, and perampanel, a non-competitive antagonist of AMPA receptors. Both drugs have been approved in Europe and the United States for the treatment of focal seizures, and perampanel is also approved for the treatment of generalized tonic-clonic seizures in patients with idiopathic generalized epilepsy. Perampanel is currently one of the mostly widely used second generation AEDs. Although retigabine has been voluntarily withdrawn from the market by the

manufacturer in June 2017 (when the work described in the present thesis had already been initiated) due its limited utilization following the discovery of unusual side effects (blue discoloration of skin, nails, conjunctiva, as well as retinal changes), interest in its utilization has been rekindled recently following reports of very promising therapeutic results in children with KCNQ2 encephalopathy, a rare but serious disorder associated with impaired neuronal potassium channel activity. Based on this background, retigabine is currently being evaluated in a Phase III clinical trial aimed at evaluating its efficacy as a precision therapy for KCNQ2 epileptic encephalopathy (Hoffman, 2019).

The pharmacokinetics of both perampanel and retigabine have not been completely characterized, and in particular there is very limited information on the factors that can affect their serum levels at steady-state. Most important, no adequate evidence is available on the relationship between the concentration of these drugs in biological fluids and clinical response in terms of seizures control and incidence/intensity of adverse effects. The importance of obtaining this information is evident in the light of the fact that both these drugs have a highly variable pharmacokinetics, a potentially high susceptibility to metabolic drug interactions, and a narrow therapeutic index (Patsalos et al., 2018). Elucidation of the factors that affect the pharmacokinetics of these agents, and characterization of the relationship between their concentration in body fluids and therapeutic response, can be important not only to improve their efficacy and safety but also to create the necessary knowledge background for a correct use of TDM in the individualization of the treatment. In the case of retigabine, it would also be particularly important to determine in future studies whether there is a threshold serum concentration below which cutaneous, mucosal and retinal adverse effects are unlikely to occur.

Many techniques can be used for the quantitation of AEDs in body fluids, either for TDM applications in the routine clinical setting or primarily for research purposes (Patsalos et al., 2008). The techniques most frequently used in many laboratories involve immunoassay procedures (fluorescence polarization immunoassay, photometric immunoassays, turbidimetric assays and chemiluminescent assays) and chromatographic techniques (gas and liquid chromatography). In the case of retigabine, available assay methods are well suited for research applications, but no assay method is available that could be conveniently applied to TDM in the routine clinical setting. For perampanel, an HPLC method applicable to TDM has been recently developed (Franco et al., 2016), but there is scope for improvement particularly with respect to making it applicable to the assay of dried plasma spots, which enhance access to

TDM by facilitating storage and shipment of samples. These unmet needs provide the rationale for part of the work described in the present thesis.

1.6.2 Characterization of miRNAs in extracellular vesicles as potential markers of drug resistance

As discussed in the section on the role of biomarkers in mechanisms of pharmacoresistance, miRNAs represent a group of key targets as potential epigenetic biomarkers, particularly in the light of evidence that miRNAs can play an important role in modulating epileptogenesis (Aronica et al., 2010; Bot et al., 2013; Gorter et al., 2014; Jimenez-Mateos et al., 2012; Kan et al., 2012; Kretschmann et al., 2015; Liu et al., 2010; Omran et al., 2012). There is also evidence that silencing certain miRNAs, such as miR-134, can exert neuroprotective effects and suppress seizures after status epilepticus in mice (Jimenez-Mateos et al., 2012).

Preliminary studies have suggested that the expression of specific miRNAs may be altered in patients with pharmacoresistant epilepsy (Wang et al 2015 a,b; Yan et al., 2017). In particular, a recent study found significant differences in the expression of miRNAs isolated from exosomes in patients with mesial temporal lobe epilepsy with hippocampal sclerosis (mTLE-HS) compared with healthy controls (Yan et al., 2017). Exosomes are small extracellular vesicles of endocytic origin with a 30 to 100 nm particle diameter that, together with microvesicles (100 nm to 1 μm particle diameter), are involved in cell to cell communication. The authors suggested that exosomal miRNAs might provide a biomarker for diagnosis and as well as a therapeutic target. To date, however, there have been no formal studies of miRNA expression in extracellular vesicles from patients with pharmacoresistant epilepsy.

The data reviewed above provide the rationale for conducting further studies on the value of miRNAs, with special reference to miRNAs circulating in extracellular vesicles, as potential biomarkers for pharmacoresistant focal epilepsy. These studies represent part of the work described in the present thesis.

1.6.3 Objectives of the work described in the present thesis

The work described in the present thesis is focused on the characterization and development of novel pharmacokinetic and epigenetic biomarkers that could assist physicians not only in

optimizing response to AEDs treatment, but also in permitting early identification of those patients who are pharmacoresistant. Specifically, the following six main objectives have been pursued:

- Develop and validate an HPLC method for the determination of retigabine in human plasma, with performance characteristics suitable for TDM purposes;
- Develop and validate an HPLC method for the determination of perampanel in dried plasma spots, with performance characteristics suitable for TDM purposes;
- Test the applicability of the above methods to TDM by measuring the concentration of both drugs in the plasma of patients receiving therapeutic dosages;
- Evaluate the abundancy and size distribution of microvesicles and exosomes obtained from the plasma of patients with pharmacoresistant epilepsy, patients with pharmacoresponsive epilepsy and healthy controls, to test for potential differences that could aid in the early prediction of resistance to drug treatment;
- Evaluate the miRNA profiles in microvesicles and exosomes obtained from the plasma of patients with pharmacoresistant epilepsy and patients with pharmacoresponsive epilepsy, to test for potential differences that could aid in the early prediction of resistance to drug treatment;
- Compare miRNA expression profiles in patients with epilepsy and healthy controls, in order to ascertain potential differences related to the disease itself rather than drug responsiveness.

2. MATERIALS AND METHODS

2.1 Development and validation of novel assay methods for the determination of recently introduced AEDs in body fluids

2.1.1 Development and validation of a novel assay method for the determination of retigabine in human plasma

2.1.1.1 Chemicals and reagents

The chemical structures of retigabine and flupirtine (internal standard) are depicted in Figure 4.

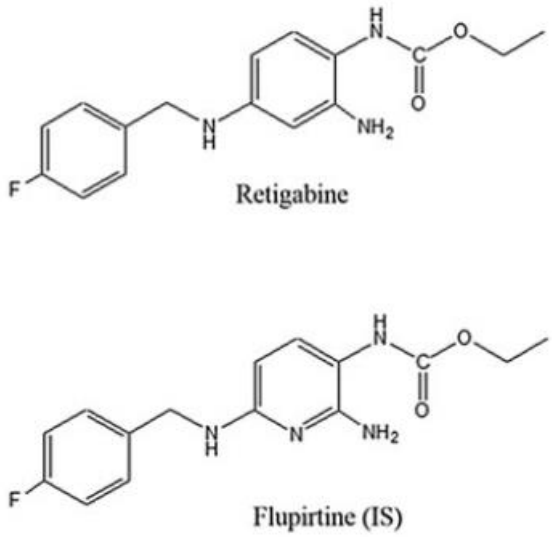

Figure 4. Chemical structure of retigabine and the internal standard flupirtine.

Retigabine, flupirtine maleate, methanol, acetonitrile and phosphoric acid 85% were purchased from Sigma Aldrich (Milan, Italy). Ultrapure water used for the mobile phase and sample solutions preparation was obtained by using a Millipore-Q-plus water purification apparatus (Millipore, Milan, Italy). Ammonium acetate solutions in water were prepared by using ammonium acetate from J.T. Baker (Deventer, The Netherlands). EMPORE High Performance Extraction Disk Cartridges (4 mm/1 mL) were from 3M Centre (St. Paul, MN, USA).

Human blank plasma, for preparation of quality control samples and calibration curves, was obtained from healthy volunteers (Immunohematology and Blood Transfusion Service, IRCCS Policlinico S. Matteo, Pavia, Italy).

2.1.1.2 Apparatus and chromatographic conditions

Assays were carried out on a Shimadzu instrument (Shimadzu Scientific Instrument Inc., Columbia, MD, USA) equipped with a System Controller SCL-10Avp, an LC-10ADvp pump, a CTO-10ASvp temperature controller, an on-line Degasser DGU-14A and a SIL-10ADvp auto injector.

The operating conditions of the instrument, optimized on the basis of the experiments conducted, were as follows:

- Column: Chromolith Performance (100 x 4.6 mm i.d., RP-18e) protected by a Chromolith guard column (5-4.6 mm i.d., RP-18e);
- λ = 240 nm (LaChrom L-7400 variable wavelength detector);
- mobile phase: water/acetonitrile/methanol (72:18:10, vol/vol/vol) mixed with 0.1% of 85% phosphoric acid (apparent pH = 2.5) in isocratic elution;
- flow rate: 1.5 mL/min;
- temperature: 50°C.

2.1.1.3 Stock solutions and quality controls

Stock solutions of retigabine (1 mg/mL) and flupirtine maleate (internal standard, 1 mg/mL) were prepared in water/acetonitrile (60/40, v/v) and methanol, respectively. Working solutions were prepared by diluting stock solutions in a mixture of water/acetonitrile (60/40, v/v) and were stable for one month at 4°C. Seven calibrators (range of calibration curve: 25-2,000 ng/mL) were prepared from blank human plasma by adding appropriate amounts of retigabine stock solution. Three quality control (QC) samples were also prepared from blank human plasma by adding appropriate amounts of retigabine stock solution to obtain concentrations of 75, 600, and 1500 ng/mL, respectively.

2.1.1.4 Sample preparation

A 300 µL aliquot of plasma was mixed with 30 µL of internal standard working solution (6.5 µg/mL) and 600 µL of ammonium acetate buffer (10 mM). After vortexing for 30 s, 800 µL of the mixture were loaded under vacuum (381 mmHg) into EMPORE Extraction Disk Cartridges

preconditioned with 1 mL of methanol, followed by 1 mL of water and 1 mL of ammonium acetate buffer. After sample loading, interfering substances were washed out with 1 mL of a mixture of 4 mM of ammonium acetate/acetonitrile/isopropylic alcohol (95:3:2, vol/vol/vol). Retigabine and internal standard were eluted with 100 µL of methanol and 150 µL of water. The eluates were vortexed for 30 s, centrifuged at 3500 rpm for 5 minutes at 4°C, transferred to a glass autosampler vial and then directly injected onto the HPLC system (50 µL).

2.1.1.5 Method validation criteria

The validation was conducted according to European Medicine Agency guidelines through the evaluation of selectivity, precision, accuracy, linearity of the calibration curves, recovery and stability (EMA guideline, 2011).

Extraction recovery was determined by comparing peak area from five different extracted QC samples with those obtained after injection of known volumes of the non-extracted solutions containing the same retigabine concentration (n = 5 for each QC).

Precision and accuracy were evaluated at three concentrations (75, 600 and 1500 ng/mL). To determine intra- and inter-day precision and accuracy, QC plasma samples were assayed in replicates on the same day (n = 5) and on three different days (n = 12, 4 for each day), respectively. Estimates of intra- and inter-day precision were expressed as coefficients of variation (CV%), with an acceptability limit set at ≤15%. Accuracy was calculated by comparison of mean assay results (n = 5 for each QC sample) with the nominal concentrations, with acceptability limits set at ±15%.

The limit of detection (LOD) was defined as the lowest concentration yielding a signal-to-noise ratio of 3, whereas the limit of quantification (LOQ) was defined as the lowest tested concentration at which CV% was <20%.

The stability of retigabine was tested by comparing baseline retigabine concentrations in freshly prepared low- and high-concentration QCs with the concentrations measured after storage in different conditions (24 hours at room temperature, 3 freeze-thaw cycles and 60 days at -30°C).

Specificity was evaluated by injecting solutions containing several drugs potentially prescribed in combination with retigabine.

2.1.1.6 Calculations and statistical analysis

Comparison among stability parameters were performed by repeated measures analysis of variance (ANOVA). A two-tailed *P*-value ≤0.05 was considered statistically significant. Statistical analyses were performed using SPSS version 20.0 (SPSS, Inc. Chicago, USA). Results were analysed using the Shimadzu LabSolution Lite software.

2.1.2 Development and validation of a novel assay method for the determination of perampanel in dried plasma spots

2.1.2.1 Chemicals and reagents

The chemical structures of perampanel and promethazine (internal standard) are depicted in Figure 5.

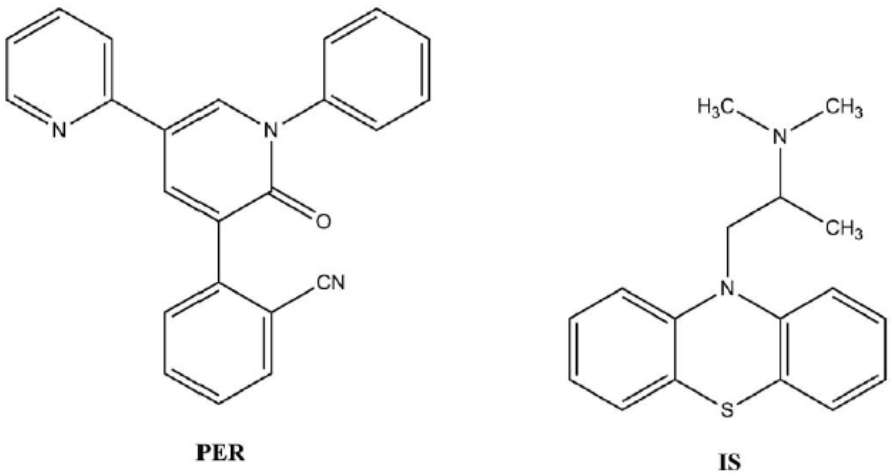

Figure 5. Chemical structures of perampanel (PER) and the internal standard promethazine (IS).

Perampanel was kindly provided by Eisai Co Ltd (Kashima, Japan). The internal standard promethazine hydrochloride, methanol and phosphoric acid 85% were obtained from Merck (Merck, Darmstadt, Germany). Acetonitrile was obtained from VWR (VWR International, Milan, Italy). Other materials used included dried sample spot devices (DSSDs, 5 cm diameter paper disks, product code DSSD-C) from Laboratori Biomicron (Laboratori Biomicron, Turin, Italy), PVDF Syringe filters (0.2 μm) from WhatmanTM (WhatmanTM, Freiburg, Germany) and ultrapure water obtained by using a Millipore-Q-plus water purification apparatus

(Millipore, Milan, Italy). Heparinized human blank plasma for preparation of QC samples and calibration curves was obtained from healthy volunteers (Immunohematology and Blood Transfusion Service, IRCCS Policlinico S. Matteo, Pavia, Italy).

2.1.2.2 Apparatus and chromatographic conditions

Assays were carried out on a Shimadzu instrument (Shimadzu Scientific Instrument Inc., Columbia, MD, USA) equipped with a System Controller SCL-10Avp, an LC-10ADvp pump, a CTO-10ASvp temperature controller, an on-line Degasser DGU-14A and a SIL-10ADvp auto injector. The Shimadzu HPLC system described above was used, with the following operating conditions:

- Column: 2 Chromolith Performance in sequence (100 x 4.6 mm i.d., RP-18e) protected by a Chromolith guard column (5-4.6 mm i.d., RP-18e);
- λ = 320 nm (LaChrom L-7400 variable wavelength detector);
- mobile phase: water/acetonitrile (60:40, v/v) mixed with 0.1% of 85% phosphoric acid in isocratic elution;
- flow rate: 1.5 mL/min;
- temperature: 50°C.

2.1.2.3 Stock solutions and quality controls

Stock solutions of perampanel and promethazine were prepared in methanol (1 mg/mL). Working solutions were prepared by diluting stock solutions in methanol for the internal standard and in a mixture of acetonitrile and water (35:65, v/v) for perampanel. These solutions were stable for one month at 4°C. Eight calibrators (i.e., 25, 50, 100, 200, 300, 500, 750, and 1000 ng/mL) were prepared from blank human plasma by adding appropriate amounts of perampanel stock solution. Three QC samples were also prepared from blank human plasma by adding appropriate volumes of perampanel stock solutions to obtain concentration of 75, 400, and 800 ng/mL.

2.1.2.4 Sample preparation

Extraction of perampanel from plasma samples was performed according to Franco et al (2016). For dried plasma spots (DPSs) a 200 µL aliquot of plasma were distributed manually on DSSD and dried at room temperature (23±2°C) for 30 minutes. DPSs were transferred in a 10 mL clear tube, and 40 µL of internal standard working solution (10 µg/mL) and 5 mL of methanol were added. After mixing for 15 minutes at room temperature, the tubes were centrifuged at 1200g for 10 minutes at 4°C. 4.3 mL of the supernatant was transferred to a clear tube and dried under air flow at room temperature. Each residue was reconstituted with acetonitrile (80 µL) and pure water (120 µL). The samples were then centrifuged, passed through a syringe filter (0.2 µm) and finally injected onto the HPLC system (50 µL).

2.1.2.5 Method validation criteria

The criteria specified for the validation of the retigabine assay (described in the previous section) method were also used for the validation of the assay of perampanel in DPSs. In addition, tests for good blood-spotting practices suggested by the European Bioanalysis Forum were performed (Timmerman et al., 2011; Timmerman et al., 2013).

Precision and accuracy (both intra-day and inter-day) were assessed for the following concentrations: 25 (LOQ), 75, 400, and 800 ng/mL.

The stability of perampanel in DPSs was evaluated by analysing extracted QC samples (n = 5, extracted for each level) at low and high concentrations exposed to different conditions including no storage (freshly prepared samples), 3 freeze–thaw cycles, storage under ambient light at room temperature for 24 hours and 1 week, as well as at -20°C (from 1 week to 3 months).

2.1.2.6 Clinical applicability and comparison with the previously published method

Plasma and DPSs samples obtained from 11 perampanel-treated patients were used to test the clinical applicability of the method and to perform a comparison between methods. A total of 23 samples were analysed. All samples were collected at steady state, approximately 12 hours after the evening dose.

2.1.2.7 Calculations and statistical analysis

Comparison among stability parameters were performed by repeated measures analysis of variance (ANOVA). A two-tailed *P*-value ≤0.05 was considered statistically significant. Passing Bablok regression analysis was used to compare perampanel concentrations measured in plasma and DPSs. Limits of agreement (LoA) were defined as the mean difference plus and minus 1.96 times the SD of the differences and acceptance limits as the 95% confidence interval (CI) of the limits of agreement. The Bland-Altman test was applied to assess the agreement between methods based on the differences between concentration values measured in DPSs and plasma and their respective means.

Statistical analyses were performed using SPSS version 20.0 (SPSS, Inc. Chicago, USA) and StataCorp statistical software version 12.0 (StataCorp-Texas, USA). Results were analysed using the Shimadzu LabSolution Lite software.

2.2 Characterization of miRNAs in extracellular vesicles as potential markers of drug resistance

2.2.1 Study design

A cross-sectional non-interventional open-label study design was used. MiRNAs profiles in extracellular vesicles derived from plasma were compared among three groups of individuals: 20 patients with drug-resistant focal epilepsy, 20 patients with drug-responsive focal epilepsy and 20 healthy control subjects. Assessment was limited to focal epilepsy in order to reduce disease-related heterogeneity, taking also into account the fact that focal epilepsy is the most prevalent type of pharmacoresistant epilepsy. As no prior information was available for power calculations, sample size was set at 20/group for exploratory purposes.

The study was conducted according to current regulations for non-profit studies and the ethical principles set out in the Declaration of Helsinki in its latest revision. The study did not affect in any way the medical management of the patients. The study protocol was approved by the ethical committee of Policlinico San Matteo in Pavia (Protocol number: P-20170034547) on December 5, 2017.

Written informed consent was obtained from all participants. Data were processed in accordance with current privacy data protection regulations.

2.2.2 Study subjects and eligibility criteria

Study subjects were enrolled according to the following eligibility criteria.

Patients with pharmacoresistant epilepsy: (i) males and females aged 18 to 65 years; (ii) an established diagnosis of focal epilepsy; (iii) currently on treatment with at least one antiepileptic drug; (iv) pharmacoresistance as defined by ILAE criteria (i.e. failure of adequate response to two tolerated and appropriately prescribed antiepileptic drugs schemes, as monotherapies or in combination, to achieve sustained seizure freedom) (Kwan et al., 2010); (v) at least 1 seizure per month on the previous 3 months while at steady state on the currently used AED regimen; (vi) absence of clinically significant medical, neurological or psychiatric comorbidity; (vii) not pregnant or breastfeeding; (viii) willingness to provide written informed consent.

Patients with pharmacoresponsive epilepsy: (i) males and females aged 18 to 65 years; (ii) an established diagnosis of focal epilepsy; (iii) currently on treatment with at least one AED; (iv) pharmacoresponsiveness as defined by ILAE criteria (i.e. freedom from seizures for at least 12 months or three times the longest pre-treatment interval between seizures, whichever is longer) (Kwan et al., 2010); (v) absence of clinically significant medical, neurological or psychiatric comorbidity; (vi) not pregnant or breastfeeding; (vii) willingness to provide written informed consent.

Healthy controls: (i) males and females aged 18 to 65 years; (ii) absence of clinically significant medical, neurological or psychiatric morbidity; (iii) not pregnant or breastfeeding; (iv) willingness to provide written informed consent.

An effort was made to ensure a comparable gender and age distribution across the three groups.

2.2.3 Plasma collection

For each subject, one blood (25 mL) sample was collected at least 3 hours after the last meal. For pharmacoresistant patients, the time elapsed since the last seizure was noted. Samples were processed at room temperature within one hour from the collection time. Cells were removed from blood samples by centrifugation at 1,000xg for 15 minutes and the supernatant was transferred in a clean tube to remove platelets and debris by additional centrifugation at 1,600xg

for 20 minutes. 1 mL of platelet-free plasma was then transferred into new tubes and stored at -80°C until analysis.

2.2.4 Isolation of extracellular vesicles

A 1.5 mL aliquot of platelet-free plasma was thawed on ice and centrifuged at 20,000xg for 1 hour at 4°C to obtain microvesicle pellets. After this step, the supernatant was transferred to a clean tube with the remaining precipitate representing the microvesicles pellets. The microvesicle pellets were then washed by resuspending the samples in sterile phosphate-buffered saline (PBS) 1X without calcium and magnesium in a final volume of 1 mL, and then centrifuged for 1 hour at 20,000xg at 4°C.

In order to obtain exosome pellets, the supernatant obtained from the first centrifugation step was filtered through 0.2 µm filter and ultracentrifuged at 100,000xg for 1 hour at 4°C (Optima Max-XP equipped with TLA55 rotor, Beckman Coulter). After supernatant discarding, the resulting exosome pellets were washed in PBS 1X without calcium and magnesium in a final volume of 1 mL, resuspended and ultracentrifuged under the same conditions reported above. The supernatant was then discarded to obtain 100 µL of exosome pellets. Microvesicle and exosome pellets were stored at -80°C until analysis.

2.2.5 Characterization of extracellular vesicles

Extracellular vesicles were characterized by different techniques to ascertain their purity, concentration and size distribution in each sample. To this aim, Western blot analysis, nanoparticle tracking analysis (NTA) and transmission electron icroscopy analysis were performed for all samples.

2.2.5.1 Western blot analysis

Total protein extraction: proteins from exosome and microvesicle pellets were extracted with a mixture containing Radio-Immunoprecipitation Assay (RIPA) buffer and phosphatase and protease inhibitors (80:10:10, v/v/v) (Sigma-Aldrich, Milan, Italy). 50 µL of each sample of exosome and microvesicle pellets were added to 50 µl of this mixture (50 mM Tris-HCl, pH

8.0, with 150 mM sodium chloride, 1.0% Igepal CA-630 (NP-40), 0.5% sodium deoxycholate, and 0.1% sodium dodecyl sulfate), incubated for 20 minutes on ice and centrifuged at 13,200xg for 20 minutes at 4°C. The resulting supernatants were transferred into fresh tubes and stored at -80°C representing the total protein extract.

Protein quantitation: protein concentration of extracted samples was determined by bicinchoninic acid (BCA) assay and bovine serum albumin (BSA) as standard. Briefly, 20 µL of a mixture containing copper (Cu^{+2}) and BCA solution (1:50 ratio) (Sigma-Aldrich, Milan, Italy), were added to 2.5 µL of the adequately diluted sample (1:15 for microvesicles and 1:20 for exosomes). After vortexing, the preparation was incubated for 30 minutes at 37°C. A blank sample was also prepared to normalize the protein quantification analysis with Nanodrop 1000 UV/VIS Spectrophotometer (Thermo Fisher Scientific, Life thecnology, US).

Western blot analysis: 30 µg of proteins were loaded on the SDS 4-15% polyacrylamide precast gel (Biorad, Milan, Italy). Laemmli buffer (0.6 g/100 mL Tris, 2 g/100 mL SDS, 10% glycerol, 1% β-mercaptoethanol, pH 6.8) was added to each sample and the mixture was incubated at 80°C for 10 minutes. Then, the samples and Precision Plus Protein™ WesternC™ (Biorad, Milan, Italy) molecular weight marker were loaded on the gel for electrophoresis for 2 hours at 120 mV. After this separation step, the proteins were transferred on a PVDF membrane with a semi-dried procedure (Trans-blot Turbo, Biorad, Milan, Italy). Before the primary antibody incubation, the membrane was blocked with 10 mL of a 5% non-fat milk prepared in TBS-T buffer (10 mM Tris-HCl, 100 mM NaCl, 0.1% Tween, pH 7.5) at room temperature for 1 h to prevent unspecific protein binding. All primary antibodies were prepared in blocking solution and were incubated overnight at 4°C in continuous shaking. Anti-Integrin-α2β was used to identify microvesicles and Anti-Alix to identify exosomes (refer to Table 1 for specifications). After primary antibody incubation, the membrane was washed in TBS-T (3 times, 10 minutes at room temperature) and incubated for one hour with adequate secondary antibodies (dilution 1:5,000) at room temperature in continuous shaking.

Table 1. Antibodies used in Western Blotting analysis.

Antibody	**Species**	**Concentration**	**Type**	**Supplier**
Anti-Integrin-α2β	Mouse	1:500	Polyclonal I Ab	Santa Cruz Biotechnology
Anti-Alix	Rabbit	1:500	Polyclonal I Ab	Abcam

A donkey anti-rabbit or an anti-mouse peroxidase-conjugated secondary antibody (GE Healthcare) were used to detect immunoreactivity and visualized with chemiluminescence detection kit (ECL Select, GE Healthcare) after membrane washing in TBS-T (3 times, 10 minutes at room temperature). Then, the primary and secondary antibodies were removed by incubation in stripping solution (100 mM mercaptoethanol, 2% SDS, and 62.5 mM Tris/HCl, pH 6.7) for 20 minutes and washed in TBS-T (3 times, 10 minutes at room temperature).

2.2.5.2 Nanoparticle tr*acking* a*nalysis*

Size and concentration of freshly prepared exosomes and microvesicles were determined using a Nanosight NS300 LM10HSBF instrument (Malvern, Amesbury, UK). This instrument uses the properties of light scattering and Brownian motion of the particles. To have an accurate sample analysis, each sample was previously diluted with filtered PBS maintained at 4°C to an optimal concentration for each sample. The number of particles per frame useful to an optimal analysis is 50 ±20, while the adequate thresholds for evaluation of exosomes and microvesicles are 3 and 5, respectively. After appropriate dilution to obtain an adequate sample concentration, 500 µL of each sample were loaded with a sterile syringe for the analysis. The detection was obtained by using a monochromatic laser beam at 488 nm and recording 3 videos of 60 s with a frame rate of about 30 frame/s for each sample. Extracellular vesicle mean size and concentration were analysed by NTA software (version 3.4, Nanosight). NTA results were reported as the mean of three independent tests. The dilution factor and the initial volume of plasma were taken into account to calculate the actual concentration of vesicles.

2.2.5.3 Transmission electron microscopy analysis

Electron microscopy analysis was performed with a JEOL JEM-1200EXIII instrument with Mega View III CCD digital camera (JOEL, Tokyo, JAPAN). 25 µL of freshly prepared

microvesicles and exosomes were fixed by mixing each sample with 175 µL of paraformaldehyde at 4%, and incubated for three hours at 4°C. A formar/carbon-coated transmission electron microscopy 200 mesh grid was placed on 50 µL of mixture for 2 min at room temperature. The grids were carefully blotted on filter paper and stained for 1 min with 2% uranyl acetate. After drying at room temperature, the grids were directly observed.

2.2.6 MiRNA isolation, sequencing and expression level analysis

Microvesicles and exosomes were extracted from 4.5 mL of plasma in accordance with the method described in the previous section ("Isolation of extracellular vesicles"). The pellets obtained from the 3 aliquots were unified before each washing steps.

2.2.6.1 Total RNA isolation

All microvesicle and exosome pellets obtained by centrifugation of 4.5 mL of plasma were used for miRNA extraction (isolation method described in "Isolation of extracellular vesicles" paragraph). Total RNA, including small RNA, was then isolated with miRNeasy Mini kit (Qiagen, Venlo, Netherlands) in accordance with the instruction manual to obtain 30 µL of extracted sample. Extracellular vesicles obtained from 2 controls, 2 pharmacoresponsive patients and 2 pharmacoresistant patients were processed at the same time. The miRNeasy Mini Kit (Qiagen, Venlo, Netherlands) was used in accordance with the instruction manual to purify total RNA from defrosted samples. The RNA isolation protocol utilizes QIAzol Lysis reagent, chloroform, and ethanol. The purification of extracts was obtained by columns and several centrifugation steps. At the end RNA was eluted with 30 µL of RNase-free water and was immediately stored at -80°C.

2.2.6.2 Library generation

To verify the quantity and quality of RNA extracted before the library construction, the samples were tested using 2100 Bioanalyzer "total RNA pico bioanalyzer kit" (Agilent, Santa Clara, CA 95051, US). The RNA samples were used to produce cDNA libraries using the Small RNA-Seq Library Prep kit (Lexogen, Greenland, US) according to the user manual. Twelve samples were processed for every library generation. Input RNA was primarily ligated to a 3' adapter

then, after removing excess 3’ adapter by column purification, it was ligated to 5’ adapter and its excess was removed. In the second step the RNA, flanked by 5’ and 3’ adapters, was converted into cDNA during the PCR amplification step through the adjunction of multiplexing indices. These indices are used to distinguish the single samples after the pooling phase. The library product cleaned-up and concentrated with a magnetic bead-based purification protocol. This step removes linker-linker artefacts (120 bp). The presence of linker-linker artifacts in the library may reduce the power of amplification and the consequent sequencing results. A Lexogen’s Purification Module with Magnetic Beads was used to achieve this goal according to the instruction manual. Lastly, the libraries were sequenced on NGS platforms (Figure 6). The sequencing step was performed with NGS technologies using Illumina Genome Analyzer and the NextSeq 500/550 High Output v2.5 kit (150 cycles) produced by Illumina. The Illumina NGS platforms make a clonal amplification with an in vitro cloning step to amplify cDNA molecule in a cell-free system.

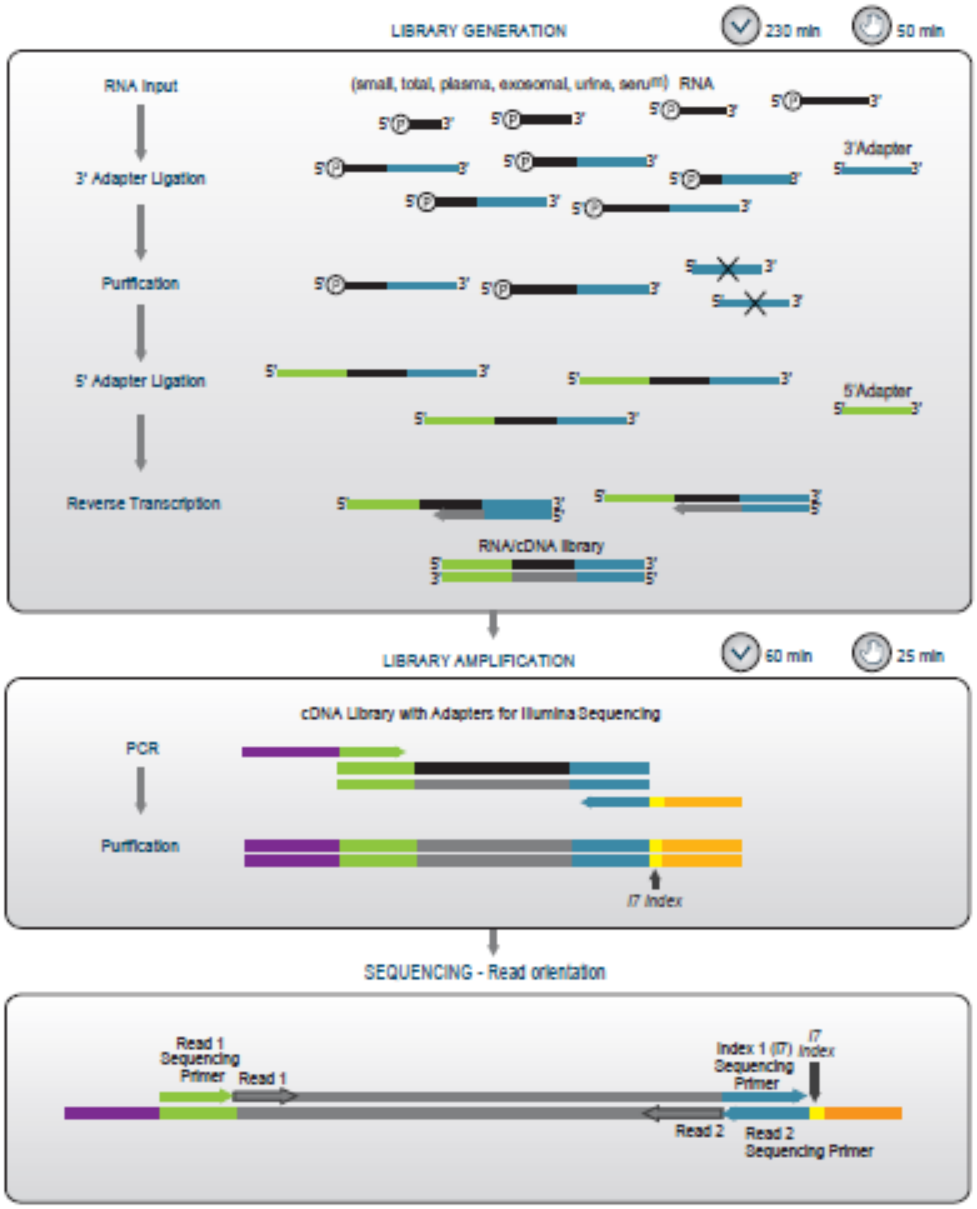

Figure 6. Library preparation workflow (Small RNA-Seq Library Prep kit - User Guide – Lexogen)

This technology performs a so-called bridge PCR amplification (Figure 7), in which the adapters linked are immobilized on glass and during PCR cycles the single-stranded cDNA fragments are annealed to them by oligonucleotide hybridization in a bridging way. At the end of the process, a population of identical templates is generated. The library was spliced into single strands with the help of linearization enzyme. Four types of nucleotides (ddATP, ddGTP, ddCTP, ddTTP) linked to a different cleavable fluorescent dye and a removable blocking-group,

were complemented to the template one base at a time. When a single ddNTP was added a fluorescent signal was produced and captured by a charge-coupled device (CCD) (Figure 7).

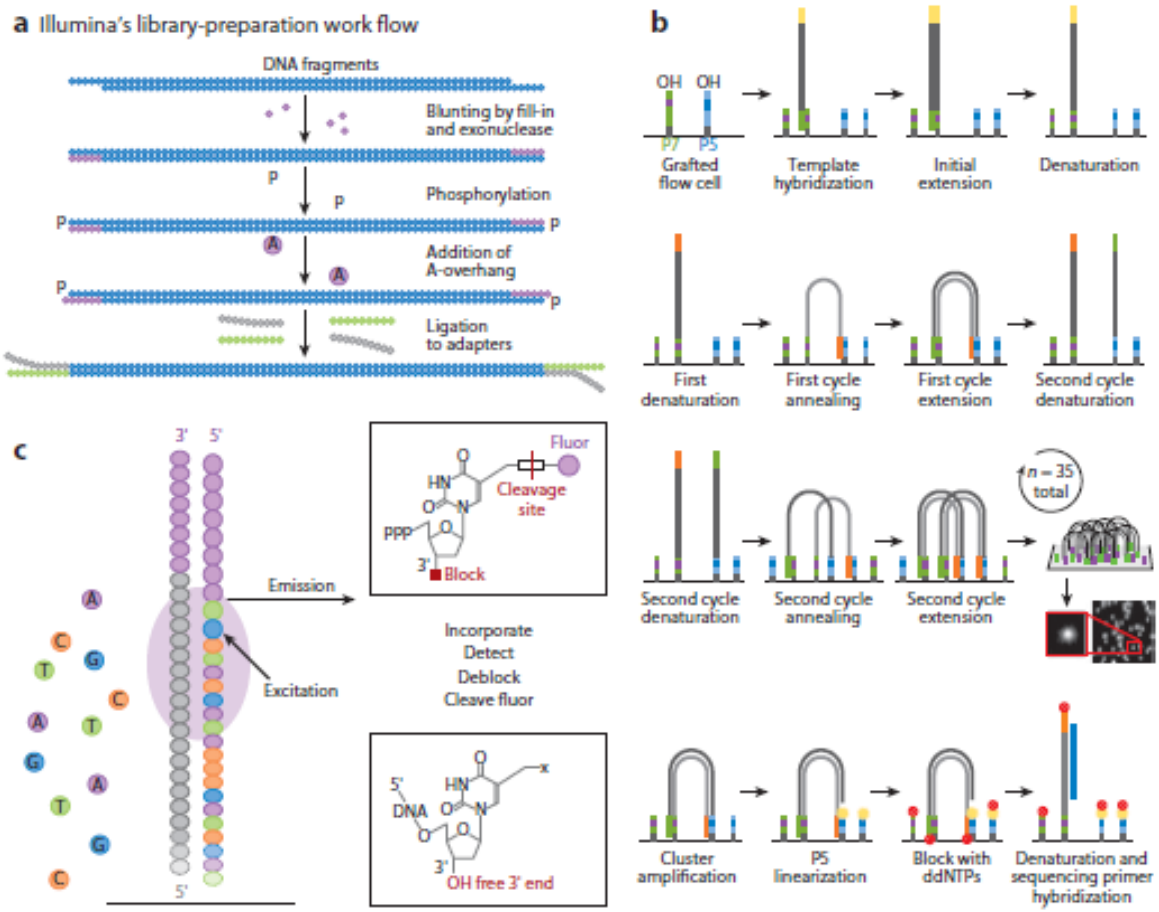

Figure 7. Representation of the amplification process with Illumina technology: a) adapters are ligated to sequence fragments; b) primer-loaded flow cells are annealed to adapters of fragments and bridge PCR reactions amplify each sequence to produce clusters of fragments; c) during the sequencing, one nucleotide ligated to a fluorophore is added to the growing strands. The fragments are sequenced when a laser excites the fluorophores and an optic scanner collects the signals from each fragment cluster. The sequencing terminator linked to each nucleotide is removed to starts the next amplification cycle (Mardis, 2013).

The sequences of nucleotides that constitute the fragments are represented by raw reads. The abundance of a transcript is in direct relation with the quantity of the generated reads. The quality of each library was assessed by 2100 Bioanalyzer with a DNA High Sensitivity assay.

Libraries were fluorometrically quantified using a High Sensitivity ds DNA assay with Qubit device. RNA processing was carried out using Illumina NextSeq 500 Sequencing. FastQ files were generated via Illumina bcl2fastq2 (Version 2.17.1.14 - http://support.illumina.com/downloads/bcl-2fastq-conversion-software-v217.html) starting from raw sequencing reads produced by Illumina NextSeq sequencer. MiRNAs were mapped on miRbase hairpins using SHRiMP. Differential expression analysis for miRNAs was performed with the R package DESeq2 (R software, Vienna, Austria). The package DESeq2 provides methods to test for differential expression by use of negative binomial generalized linear models; the estimates of dispersion and logarithmic fold changes incorporate data-driven prior distributions (Love et al., 2014). MiRNAs with more than 5 counts were retained for further analysis. We considered as differentially expressed miRNA with |log2(disease sample/healthy control)| ≥ 1 and a FDR ≤ 0.1. We set a minimum |Log2FC| of 1 and an FDR lower than 0.1 as thresholds to differentially expressed genes to maximize the sensitivity of this analysis and in order to perform a massive screening and identify candidate miRNAs.

2.2.6.3 Pathway analysis

The involvement of identified miRNAs in potential epilepsy-related pathways (predicted target genes and predicted pathways) has been investigated with the miRWalk 3.0 database. This tool contains a list of miRNAs previously associated with many diseases. MiRNAs that were found to be deregulated in our study were searched in the lists of miRNAs present in “epilepsy”, “temporal lobe epilepsy”, and “intractable epilepsy” categories in order to test for their involvement in epilepsy. A second search was conducted by using the Kyoto Encyclopedia of Genes and Genomes (KEGG) database. The genes that were found to be associated with selected miRNAs with a score prediction of 1 or a p-value <0.5 were considered for a pathway analysis.

3. RESULTS

3.1 Development and validation of novel assay methods for the determination of recently introduced AEDs in body fluids

3.1.1 Development and validation of a novel assay method for the determination of retigabine in human plasma

3.1.1.1 Chromatographic separation

Under the chromatographic conditions described in the "Materials and methods" section, the retention times of flupirtine and retigabine were 2.7 and 3.2 minutes respectively, while the total duration of the chromatographic run was 7 minutes. Representative chromatograms of a blank plasma sample, a quality control sample and a plasma sample from a patient treated with retigabine are illustrated in Figure 8.

3.1.1.2 Method validation

Accuracy values were within the 99.7% to 108.7% range, while intra–day and inter-day CVs values were lower than 12.6% (Table 2). The mean recovery ranged from 95.6% to 99.8%.

Calibration curves showed a good linearity over the whole calibration range (25-2000 ng/mL), with correlation coefficients higher than 0.998. LOD and LOQ values were 10 ng/mL and 25 ng/mL, respectively. The LOQ for inter-day accuracy was 104.2%, while inter-day precision was 12.6%. The mean back-calculated concentrations of calibration standards are reported in Table 3.

Stability data are reported in Table 4. No significant differences in retigabine concentration were observed when samples were stored at 24 h at room temperature, after three freeze/thaw cycles and for up 60 days at -30°C (repeated measure ANOVA, NS).

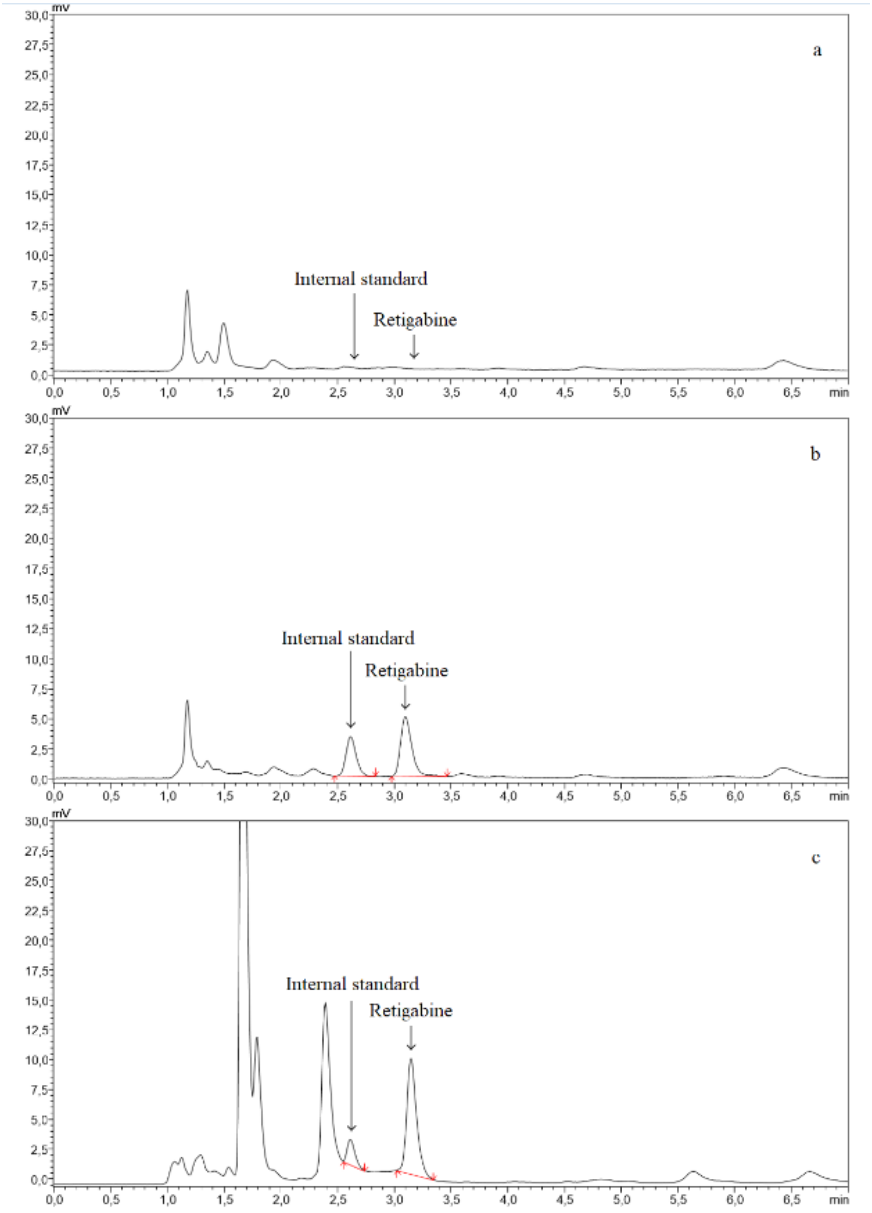

Figure 8. Representative chromatograms of a blank plasma sample (a), a quality control sample containing retigabine 600 ng/mL (b), and a sample from a patient taking retigabine 750 mg/day (c). Co-administered AEDs for the patient included in this study were ethosuximide 1500 mg/day, lamotrigine 175 mg/day and valproic acid 2000 mg/day. The retigabine concentration in the patient's sample was 1240 ng/mL.

Table 2. Interday and intraday precision and accuracy in the quantitation of retigabine in human plasma.

Assay	Nominal concentration (ng/mL)	Mean measured concentration (ng/mL)	CV (%)	Accuracy (%)
Intra-assay (n=5)	25	27.2	1.7	108.7
	75	79.4	4.4	105.9
	600	631.5	1.6	105.2
	1500	1600.4	1.8	106.7
Inter-assay (n=12)	25	26.0	12.6	104.2
	75	74.8	8.1	99.7
	600	634.0	6.9	105.7
	1500	1527.2	5.2	101.8

Table 3. Back calculation analysis of calibrators.

Back calculation (n=3)	Nominal concentration (ng/mL)						
	25	**50**	**200**	**400**	**800**	**1400**	**2000**
Mean	26.0	46.4	200.9	392.6	800.0	1415.6	1999.2
SD	3.5	4.4	5.0	24.9	22.3	24.5	7.9
CV (%)	13.6	9.5	2.5	6.3	2.8	1.7	0.4
Accuracy (%)	103.8	92.9	100.4	98.2	100.0	101.1	100.0

Table 4. Retigabine stability in plasma under different storage conditions

Storage condition	Nominal concentration (ng/mL)	Mean measured concentration (ng/mL) ± SD	95% Confidence Intervals
Freshly prepared samples			
	75	69.8±5.9	75.3-64.3
	1500	1481.9±51.8	1530.1-1433.7
24 h at room temperature			
	75	71.6±3.5	74.8-68.4
	1500	1501.4±66.4	1563.1-1439.7
3 freeze-thaw cycles			
	75	68.9±1.1	70.0-67.9
	1500	1485.5±16.3	1500.6-1470.3
60 days at -30°C			
	75	69.2±3.8	72.8-65.7
	1500	1491.5±34.9	1523.8-1458.9

No interfering peaks were detected in chromatograms obtained after extraction of 6 blank plasma samples from healthy volunteers. Potential interference from potential concomitantly administered AEDs, the main retigabine metabolite (N-acetyl retigabine) and some anti-inflammatory drugs were tested by injection of 50 μL of solutions containing 5 μg/mL of each compound. The tested compounds included are reported in Table 5.

Mono-hydroxy-carbazepine was the only compound with a retention time closer to that of the internal standard. Samples derived from patients co-medicated with AEDs metabolized to mono-hydroxy-carbazepine (e.g. oxcarbazepine and eslicarbazepine acetate) can be analysed by replacing the water contained in the mobile phase with potassium hexafluorophosphate 50 mM.

Table 5. Retention time of drugs and drug metabolites tested for possible interference in the quantitation of retigabine in human plasma.

Drug or metabolite	**Retention time (min)**
Carbamazepine	6.7
Carbamazepine-10,11-diol (metabolite of carbamazepine)	2.2
Carbamazepine-10,11-epoxide (metabolite of carbamazepine)	3.7
Diazepam	12.4
Ethosuximide	ND
Felbamate	ND
Gabapentin	ND
Ibuprofen	ND
Lamotrigine	1.6
Levetiracetam	ND
Lorazepam	2.5
Mono-hydroxy-carbazepine (metabolite of oxcarbazepine and eslicarbazepine acetate)	2.8
Nitrazepam	ND
Nortriptyline	11.7
N-acetyl retigabine (metabolite of retigabine)	1.7
Oxcarbazepine	4.3
Paracetamol	1.4
Phenytoin	6.2
Phenobarbital	3.0
Prednisolone	5.6
Pregabalin	ND
Risperidone	ND
Rufinamide	2.2
Topiramate	ND
Valproic acid	ND
Vigabatrin	ND
Zonisamide	2.0

ND = not detected

3.1.2 Development and validation of a novel assay method for the determination of perampanel in dried plasma spots

3.1.2.1 Chromatographic separation

Under the chromatographic conditions described in the "Materials and methods" section, optimal separation of perampanel and the internal standard was obtained with peak retention times of 2.75 minutes for the internal standard promethazine and 4.8 minutes for perampanel. Representative chromatograms of a DPS blank sample and a DPS prepared using a quality control sample (perampanel 400 ng/mL) are shown in Figure 9.

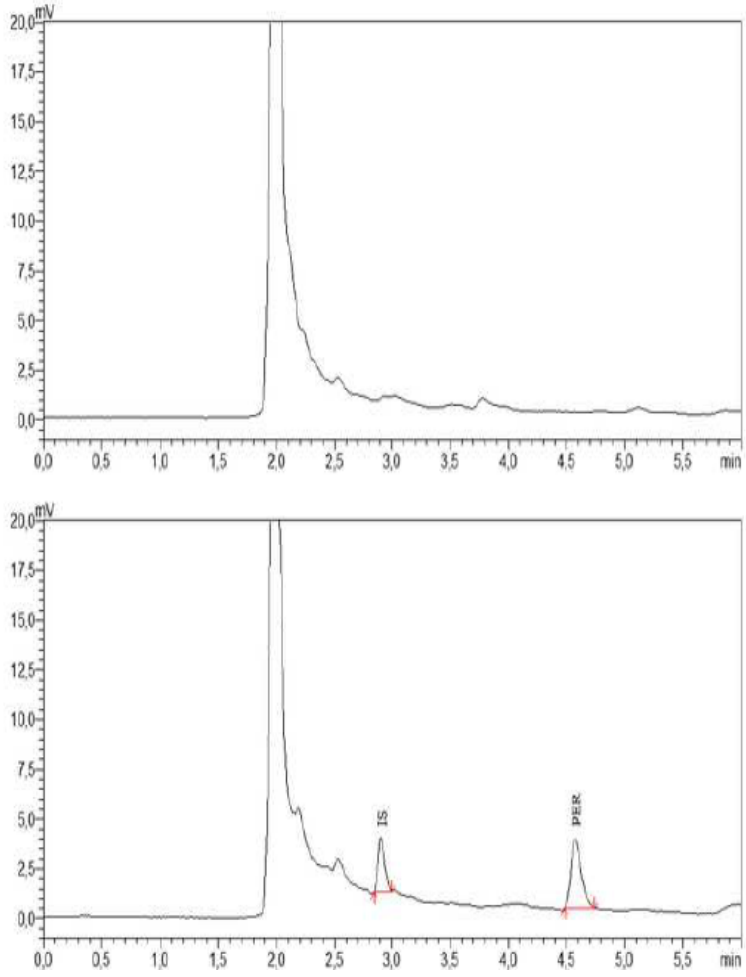

Figure 9. Representative chromatograms of a DPS blank sample (top panel) and an extracted DPS quality control sample (400 ng/mL) (lower panel).

3.1.2.2 Method validation

Accuracy values were within the 99.2% to 111.4% range, while intra-day and inter-day CV values were below 15% (Table 6). The mean recovery from human DPSs ranged from 81% to 90%.

Table 6. Intra-day and inter-day precision and accuracy of measured DPS perampanel concentration (n = 5 for each concentration). QC = Quality control sample.

	Intra-day			**Inter-day**		
Nominal concentration	**Mean measured concentration (ng/mL) ±SD**	**CV (%)**	**Accuracy (%)**	**Mean measured concentration (ng/mL) ±SD**	**CV (%)**	**Accuracy (%)**
LOQ (25 ng/mL)	26.1±2.1	8.1	104.5	27.5±1.7	6.2	109.9
QC1 (75 ng/mL)	78.4±2.2	2.8	104.6	74.4±5.1	6.9	99.2
QC2 (400 ng/mL)	445.6±15.0	3.4	111.4	420.3±36.1	8.6	105.1
QC3 (800 ng/mL)	856.9±58.2	6.8	107.1	823.9±49.5	6.0	103.0

Calibration curves were linear over the concentration range tested (25-1000 ng/mL). Coefficients of correlation of the curves were higher than 0.998 and slopes were 0.0045±0.0002. The LOD and LOQ were 10 ng/mL and 25 ng/mL respectively.

No significant perampanel loss was observed at room temperature (1 day and 1 week), after three freeze/thaw cycles and after 1 week and 3 months at -20°C (repeated measure ANOVA, NS) (Table 7). No interference from other commonly co-prescribed drugs were observed with this method at the retention times of perampanel and the internal standard. No carry-over was detected for perampanel and the internal standard.

Table 7. Stability of perampanel in the low quality control sample (75 ng/mL) and the high quality control sample (800 ng/mL) (n = 5 for each experiment) under different storage conditions.

Storage condition	**Nominal concentration (ng/mL)**	**Mean measured concentration (ng/mL)±SD**	**Nominal concentration (ng/mL)**	**Mean measured concentration (ng/mL)±SD**
Controls	75	77.8±8.4	800	822.77±27.7
24 hours at room temperature	75	85.2±0.9	800	851.5±16.6
1 week at room temperature	75	77.2±5.9	800	786.7±35.7
3 freeze/thaw cycles	75	78.7±4.9	800	799.9±17.1
1 week at – 20° C	75	79.4±4.2	800	827.6±28.5
3 months at –20°C	75	77.0±3.1	800	758.1±71.4

3.1.2.3 Clinical applicability and comparison with the previously published method

Perampanel levels measured in plasma and DPSs obtained from one patient assessed at three different dosage levels are illustrated in Figure 10. A total of 18 additional samples (DPS and plasma) obtained from 10 patients were assayed.

Plasma and DPS concentrations of perampanel in 23 samples were compared using Passing-Bablok regression analysis. No systematic constant/proportional error was identified (Figure 11A). The regression curve (95% CI) had a slope -3.06 (range, -16.67 to 10.17). The intercept was 0.99 (0.95 to 1.03). No statistical difference emerged between data obtained with plasma and DPSs (Lin's concordance correlation coefficient: 0.996; Cusum test p-value: >0.20). Likewise, no significant differences between plasma and DPS assay values were detected by the Bland-Altman plot (Figure 11B).

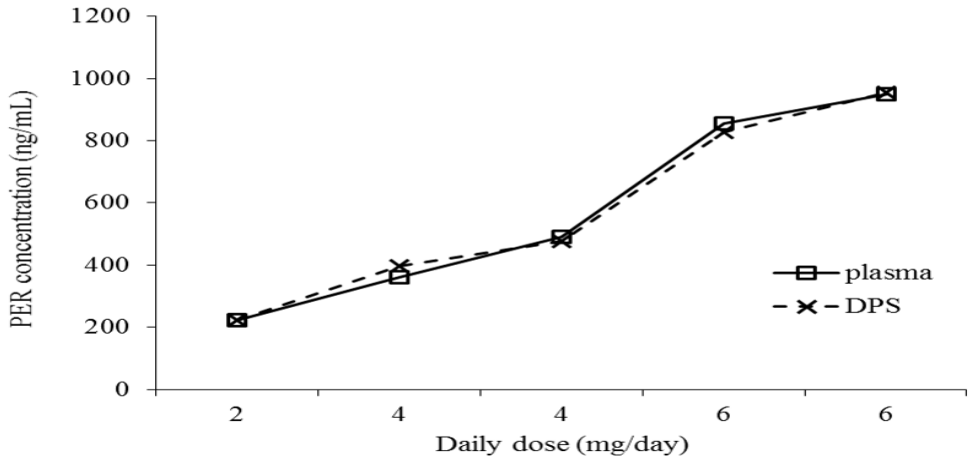

Figure 10. Perampanel (PER) concentrations in plasma and DPS samples from a patient receiving perampanel and assessed at three different dose levels (2, 4 and 6 mg/day).

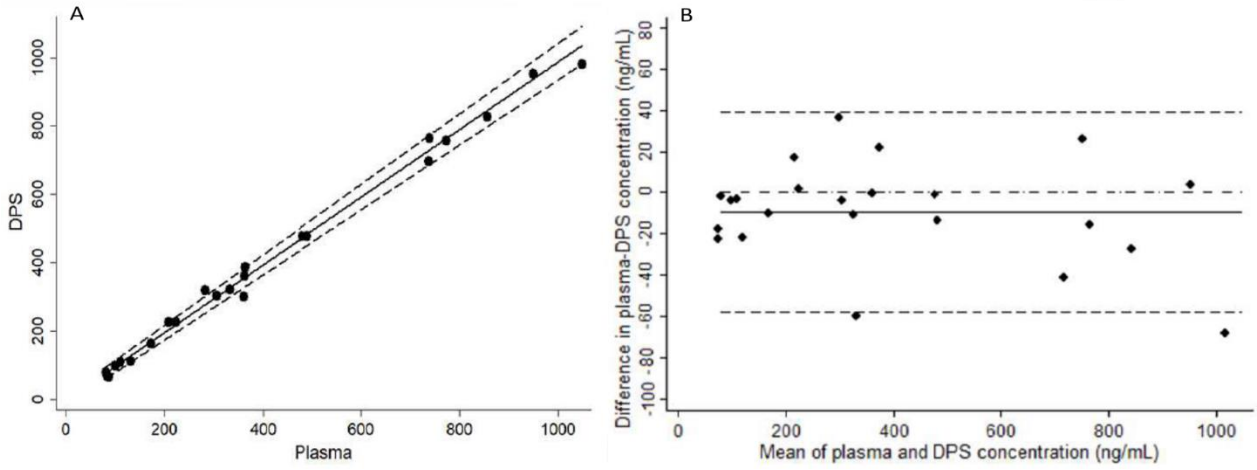

Figure 11. (A) Passing-Bablok correlation plot of perampanel concentrations measured in plasma and DPS samples (n = 23). The dotted lines represent 95% confidence intervals (CI). (B) Bland-Altman plot of mean perampanel concentrations measured in plasma and DPS samples (n = 23) (x-axis) versus the difference between plasma and DPS concentrations (Y-axis). The continuous line represents the proportional difference (bias=-9.43; 95% CI:-20.05;1.20). Dotted lines represent the lower limits of agreement (LoA) (95% CI:-57.58;-75.99 to -39.18) and the upper LoA (95% CI:38.73; 20.33 to 57.13). The fitted regression line with 95% CI is represented by the dotted line close to the bias.

3.2 Characterization of miRNAs in extracellular vesicles as potential markers of drug resistance

3.2.1 Characteristics of the study population

A total of 60 subjects (20 pharmacoresponsive patients, 20 pharmacoresistant patients and 20 healthy controls) were enrolled. Demographic and other clinical characteristics of pharmacoresponsive and pharmacoresistant patients are given in Tables 8 and 9 respectively. Mean age (± SD) was 42 ± 14 years for the pharmacoresponsive patients group, 48 ± 11 years for the pharmacoresistant patients group and 43 ± 14 years for the healthy controls. Gender distribution (males/females) was 11/9 for the pharmacoresponsive patients group, 11/9 for the pharmacoresistant patients group and 9/11 for the healthy controls.

The large majority of pharmacoresponsive patients had focal epilepsy of unknown aetiology (80%), with only 4 subjects having amygdala or hippocampal abnormalities or post-vasculitic changes. Among the pharmacoresistant patients, aetiology was unknown in 10 cases and structural in the remaining patients. Of pharmacoresponsive patients, 85% were on monotherapy, while in the pharmacoresistant group only 5% were treated with a single AED.

Table 8. Demographic and disease-related characteristics of the patients with pharmacoresponsive epilepsy included in the study. CBZ, carbamazepine; LCM, lacosamide; LEV, levetiracetam; LTG, lamotrigine; OXC, oxcarbazepine; PB, phenobarbital.

Patient	**Age**	**Gen-der**	**Aetiology**	**Seizure type**	**Drug treatment (mg/day)**
1	42	F	Dysplasia of amygdala dysplasia and malformation of the head of the hippocampus	Focal aware seizures and bilateral tonic-clonic seizures	CBZ (700)
2	40	M	Unknown	Focal aware seizures and bilateral tonic-clonic seizures	LEV (2000)
3	42	F	Unknown	Focal impaired awareness seizures	CBZ (600)
4	54	F	Sequelae of cerebral vasculitis	Focal aware seizures	CBZ (400)
5	20	F	Unknown	Focal impaired awareness seizures	CBZ (400)
6	52	F	Unknown	Focal aware seizures and bilateral tonic-clonic seizures	LEV (3000) LAC (300)
7	20	F	Hippocampal sclerosis (left)	Focal impaired awareness seizures and bilateral tonic-clonic seizures	OXC (1200) LEV (2000)
8	18	F	Unknown	Focal aware seizures	CBZ (600)
9	45	F	Hippocampal sclerosis (right)	Focal impaired awareness seizures and bilateral tonic-clonic seizures	CBZ (600)
10	31	M	Unknown	Focal aware seizures and bilateral tonic-clonic seizures	CBZ (400)
11	60	M	Unknown	Focal impaired awareness seizures and bilateral tonic-clonic seizures	LCM (300)
12	64	M	Unknown	Focal impaired awareness seizures and bilateral tonic-clonic seizures	OXC (600)
13	50	M	Unknown	Focal aware seizures and bilateral tonic-clonic seizures	CBZ (200)
14	19	M	Unknown	Focal aware seizures and bilateral tonic-clonic seizures	LEV (2000) OXC (600)
15	47	M	Unknown	Focal aware and impaired awareness seizures and bilateral tonic-clonic seizures	CBZ (600) LTG (500)
16	51	M	Unknown	Focal aware seizures and bilateral tonic-clonic seizures	PB (100)
17	49	M	Unknown	Focal aware seizures and bilateral tonic-clonic seizures	CBZ (400)
18	51	M	Unknown	Focal aware seizures and bilateral tonic-clonic seizures	CBZ (400)
19	53	M	Unknown	Focal aware seizures and bilateral tonic-clonic seizures	CBZ (400)
20	32	F	Unknown	Focal aware seizures and bilateral tonic-clonic seizures	CBZ (600)

Table 9. Demographic and disease-related characteristics of the patients with pharmacoresistant epilepsy. CBZ, carbamazepine; CLB, clobazam; LCM, lacosamide; LEV, levetiracetam; LTG, lamotrigine; PB, phenobarbital; PER, perampanel; PGB, pregabalin; PHT, phenytoin; PRM, primidone; TPM, topiramate; VPA, valproic acid; ZNS, zonisamide.

Patient	**Age**	**Gender**	**Aetiology**	**Seizure type**	**Seizure frequency***	**Drug treatment (mg/day)**
1	42	F	Unknown	Focal aware seizures and bilateral tonic-clonic seizures	6	CLB (30), LTG (200) PB (50), VPA (1300)
2	40	M	Left hippocampal sclerosis	Focal aware seizures and bilateral tonic-clonic seizures	2	CBZ (1200), LEV (3000), ZNS (100)
3	42	F	Unknown	Focal aware seizures and bilateral tonic-clonic seizures	3	LCM (300), VPA (600)
4	54	F	Unknown	Focal aware seizures and bilateral tonic-clonic seizures	2	LCM (350), PB (50) PER (4), VPA (1250)
5	20	F	Malformation of cortical development	Focal aware seizures and bilateral tonic-clonic seizures	9	CLB (20), LAC (400) PER (4), PGB (450) TPM (400)
6	52	F	Unknown	Focal impaired awareness seizures and bilateral tonic-clonic seizures	5	LCM (450), PER (6) PGB (300)
7	20	F	Sequelae of meningoencephalitis	Focal impaired awareness seizure and bilateral tonic-clonic seizures	3	LCM (500), LEV (2000)
8	18	F	Cerebral malformation	Focal aware seizures	4	CBZ (1800), PHT (250), PGB (300) PRM (1250)
9	45	F	Unknown	Focal aware seizures and bilateral tonic-clonic seizures	30	LCM (400), LTG (600), PER (12)
10	31	M	Right mesial temporal sclerosis	Focal impaired awareness seizures and bilateral tonic-clonic seizures	4	LEV (4000), LTG (450)
11	60	M	Unknown	Focal impaired awareness seizures and bilateral tonic-clonic seizures	4	CBZ (800), CLB (10) LCM (100), LEV (3000), LTG (400)
12	64	M	Unknown	Focal aware seizures	3	CLB (10), LEV (3000) PB (100), ZNS (300)
13	50	M	Amyloid angiopathy	Focal aware seizures and bilateral tonic-clonic seizures	2	LCM (400), LEV (2250)
14	19	M	Malacic sequelae left temporal lobe	Focal aware seizures and bilateral tonic-clonic seizures	2	LCM (500), ZNS (300)

Patient	Age	Gender	Aetiology	Seizure type	Seizure frequency*	Drug treatment (mg/day)
15	47	M	Hippocampal sclerosis	Focal aware seizures and bilateral tonic-clonic seizures	2	LCM (500), LEV (3000)
16	51	M	Left hippo-campal sclerosis	Focal aware seizures and bilateral tonic-clonic seizures	3	LCM (400), LEV (3000), PB (150) ZNS (250)
17	49	M	Unknown	Focal aware seizures and bilateral tonic-clonic seizures	1	LCM (400), LEV (2000), VPA (1000)
18	51	M	Left mesial temporal sclerosis	Focal aware and impaired awareness seizures and bilateral tonic-clonic seizures	2	CLB (20), LCM (300), PER (8), PGB (300)
19	53	M	Unknown	Focal aware seizures	3	CBZ (800)
20	32	F	Unknown	Focal aware and impaired awareness seizures and bilateral tonic-clonic seizures	2	LCM (400), VPA (500)

*Mean number of seizures per month during the previous 3 months.

3.2.2 Characterization of extracellular vesicles

The results of the characterization of exosomes and microvesicles by Western blot, nanoparticle tracking analysis, and transmission electron microscopy analysis are reported below. The protocols are chosen in accordance with guidelines proposed by the International Society for Extracellular Vesicles (ISEV) (Thery et al., 2018).

3.2.2.1 Western blot analysis

No microvesicle contamination was found in exosome pellets based on results of the Western blot experiment using Integrin α2β as marker for microvesicles. Acceptable exosome contamination was observed in microvesicle pellets with the selected exosome marker Alix. This is in line with evidence previously reported in the literature using different centrifugation steps to separate extracellular vesicles (Thery et al., 2018). A representative Western blot is reported in Figure 12.

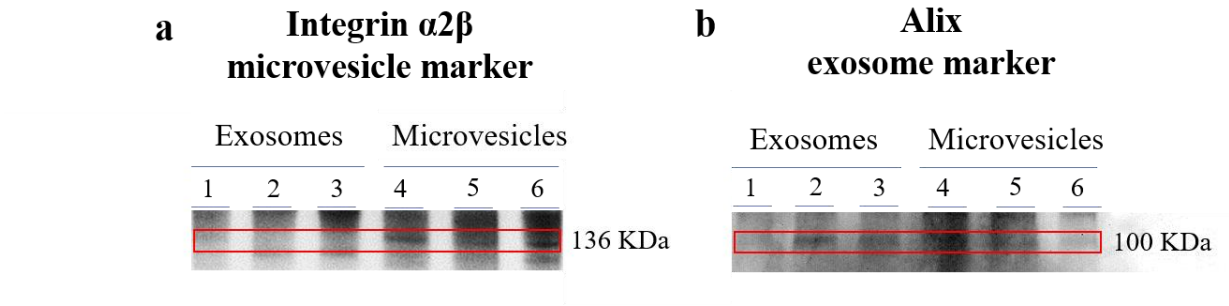

Figure 12. Western blot analysis of plasma-derived exosomes and microvesicles from one healthy control (1 and 4, respectively), one patient with pharmacoresponsive epilepsy (2 and 5, respectively) and one patient with pharmacoresistant epilepsy (3 and 6, respectively) using the microvesicle marker integrin α2β (a), and the exosome marker Alix (b).

3.2.2.2 Nanoparticle tracking analysis

Nanoparticle tracking analysis was performed in all samples as described in the "Materials and methods" section. Firstly, the size distribution in exosomes and microvesicles in each group was evaluated to confirm the low degree of overlap between the two populations of extracellular vesicles (Figure 13).

Outliers for each group (defined as those exceeding 2 SDs from the mean) were excluded from the statistical analyses. For exosomes, mean size was 70.1±8.1 nm in controls, 73.1±16.5 nm in pharmacoresponsive patients and 72.4±13.1 nm in pharmacoresistant patients; mean count was $4.2x10^{10}±2.5x10^{10}$ in controls, $4.5x10^{10}±2.6x10^{10}$ in pharmacoresponsive patients and $3.8x10^{10}±2.3x10^{10}$ in pharmacoresistant patients. For microvesicles, mean size was 114.1±32.5 nm in controls, 109.5±26.4 nm in pharmacoresponsive patients and 124.5±23.1 nm in pharmacoresistant patients; mean count was $2.7x10^{9}±1.2x10^{9}$ in controls, $3.8x10^{9}±3.3x10^{9}$ in pharmacoresponsive patients and $3.2x10^{9}±2.2x10^{9}$ in pharmacoresistant patients. The Kruskal-Wallis test was used to assess statistical differences among the three groups and no significant differences were found for either size or count. Dot plot representation of these data, however, suggests a greater variability in patients compared to controls (Figure 14).

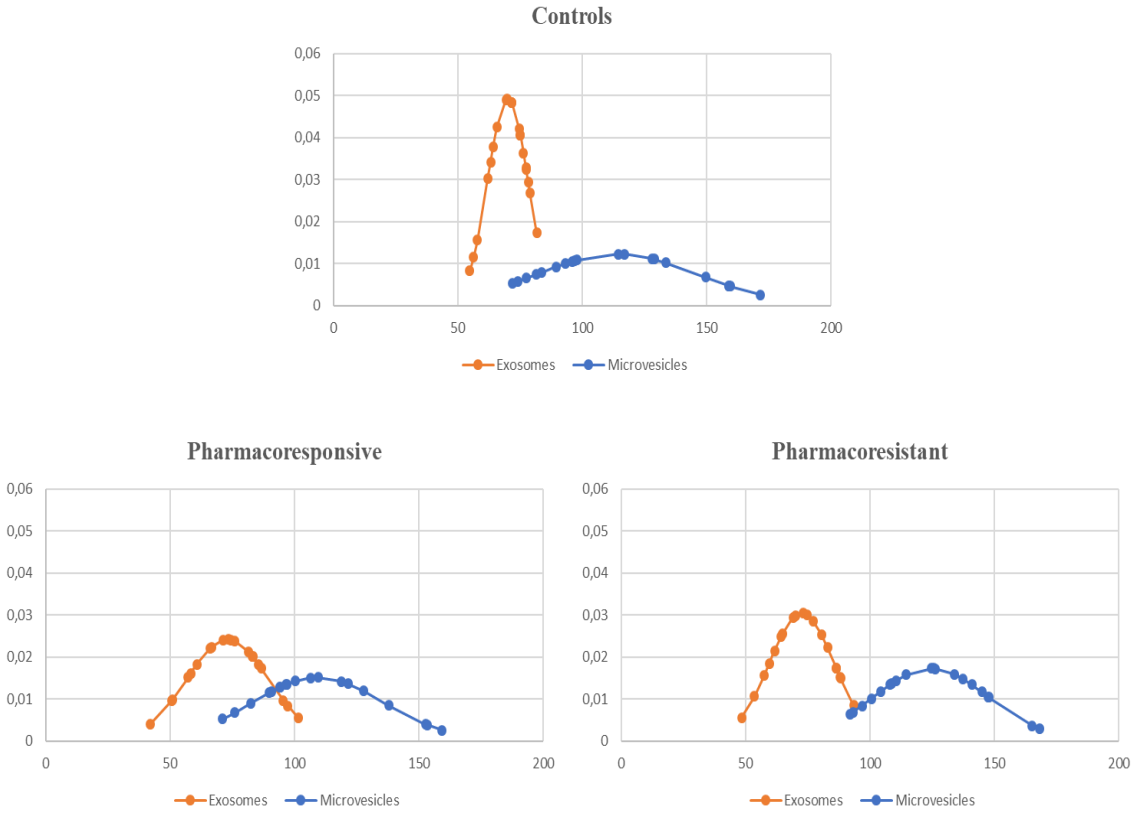

Figure 13. Distribution analysis of the size of exosomes and microvesicles in each of the three study groups.

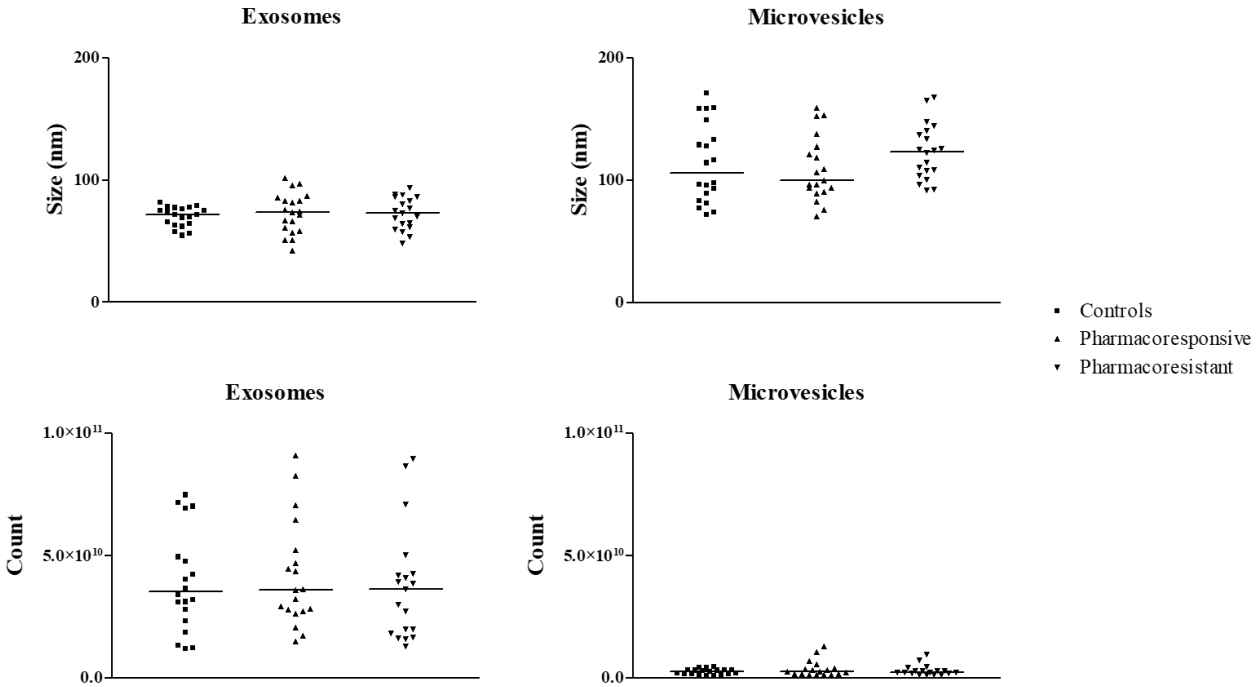

Figure 14. Dot plot representations of size and count distributions of exosomes and microvesicles in each study group. Sample size was 19 in each group, except for exosomes size in pharmacoresponsive patients (n = 20) and microvesicles size in pharmacoresistant patients (n = 20).

3.2.2.3 Transmission electron microscopy analysis

Microvesicle and exosome pellets obtained with the procedure described in the "Materials and methods" section were freshly prepared and immediately examined by transmission electron microscopy. Representative images of exosomes and microvesicles derived from controls and patients are reported in Figure 15. No differences in morphology were observed among groups. In all subjects examined, the mean size of exosomes were smaller than that of microvesicles.

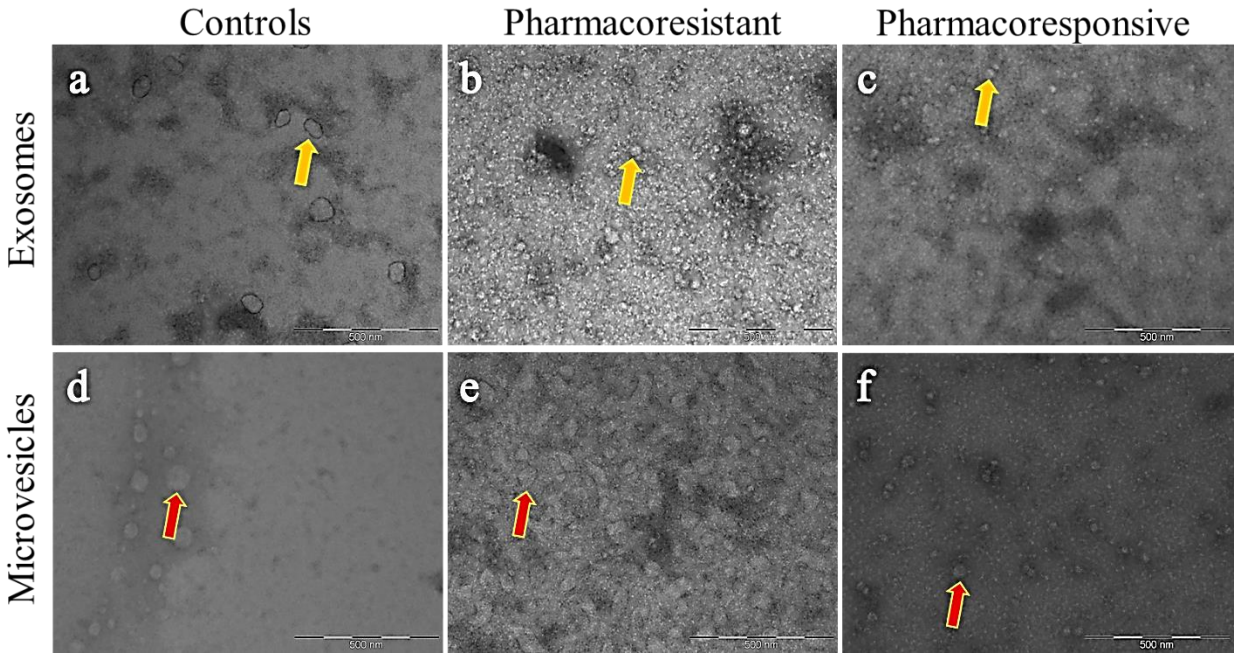

Figure 15. Representative images of exosomes and microvesicles obtained by transmission electron microscopy in one control, one patient with pharmacoresistant epilepsy and one patient with pharmacoresponsive epilepsy. Scale bar = 500 nm. Exosomes are shown in a, b, c panels respectively and microvesicles in d, e, f panels respectively.

3.2.2.4 MiRNA isolation, sequencing and expression level analysis

Three platforms NGS were used for miRNA amplification. MiRNAs extracted from exosomes and microvesicles obtained from 4 pharmacoresistant patients, 4 drug-responsive patients and 4 healthy subjects were processed for each platform. A total of 12 subjects per group were analysed for the number of reads obtained after NGS amplification. A representation of the number of reads obtained for each sample with the three Illumina platforms is reported in Figure 16. Samples with a number of reads less than 300,000 were excluded. The threshold usually applied in NGS analysis is higher (4-5 million reads as indicated in FAQ on Lexogen website, https://www.lexogen.com/small-rna-seq-library-prep-kit/) than that used in our experiments, but this cut-off was selected due to the low amount of sample obtained from isolation of microvesicles. The quality of samples that may influence the quality of results (Kolanowska et al., 2018) was previously tested. Exclusion of these miRNA reads removed potential artifacts obtained from comparison of miRNAs.

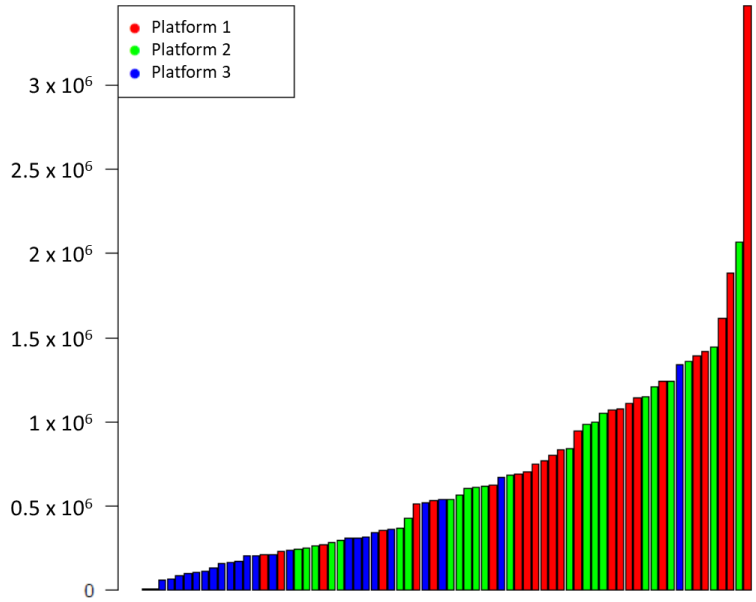

Figure 16. Graphical representation of the number of reads obtained for each sample analysed with NGS Illumina platforms. The colour of the bars represents the different cartridges used.

A total of $1.97x10^8$ processed reads for exosomes and $1.87x10^8$ for microvesicles were obtained with an average of $8.97x10^6$ and $8.48x10^6$ single-end reads per sample, respectively. Of these, 481 and 470 known miRNAs were identified in exosome and microvesicles respectively, which comprised 4.5% of total reads in both groups. The analysis shows differentially expressed miRNAs (down-regulated or up-regulated) in exosome and microvesicle heatmaps.

MiRNA expression profiles in exosomes were evaluated in 8 controls versus 7 pharmacoresistant patients, and in 8 controls versus 8 pharmacoresponsive patients. Likewise, miRNA expression profiles in microvesicles were evaluated 7 controls versus 9 pharmacoresistant patients and 7 controls versus 10 drug-responsive patients. A principal component analysis (PCA) did not evidence a strong clusterization of the three study groups (Figure 17). There was a generally low difference in the expression of all miRNAs across groups in exosomes and microvesicles. In addition, a partial clustering for pharmacoresistant patients (panel a) was detected. The heat maps constructed with the same data confirmed these results (Figure 18). Only in the heat map representing exosome-derived miRNAs it was possible to identify four areas (white or light blue) that indicated a partial clustering among groups. The

prevalent heterogeneous distribution of the three groups was clearly represented by three different colours in the top of the figure for both types of extracellular vesicles.

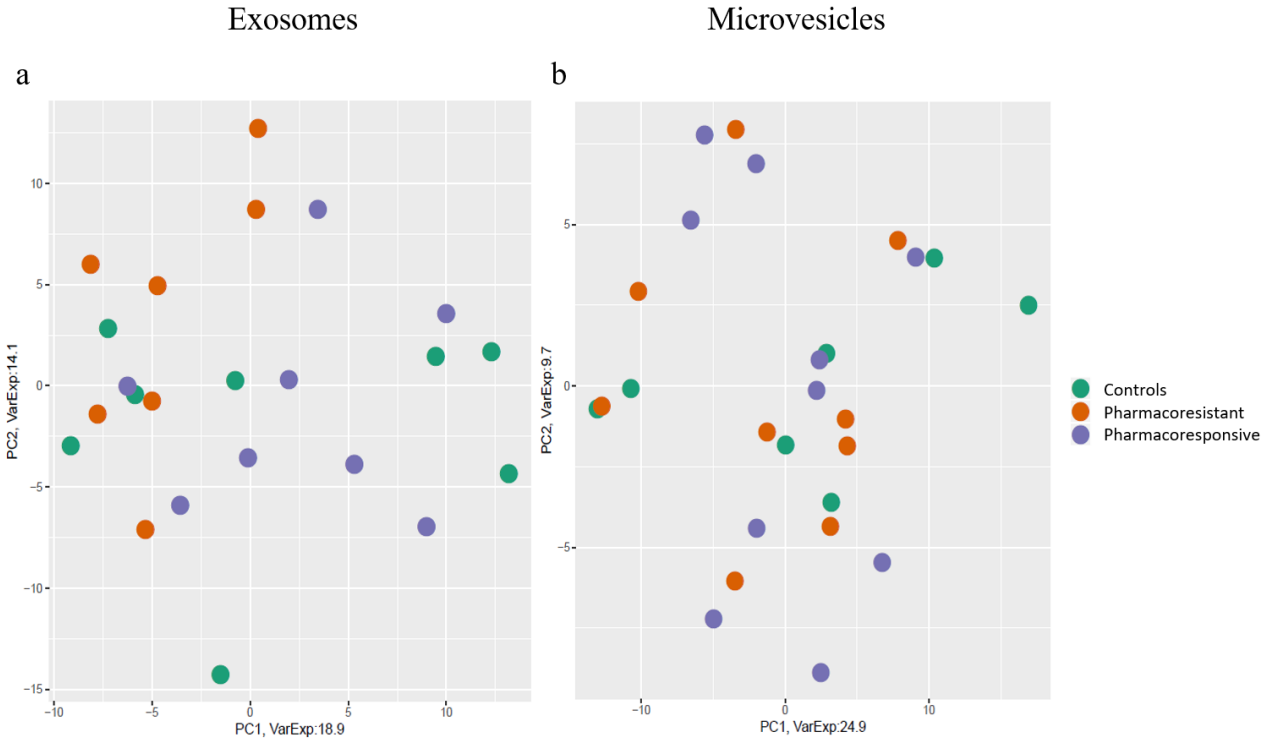

Figure 17. PCA analysis in exosomes (a) and microvesicles (b) in the three study groups.

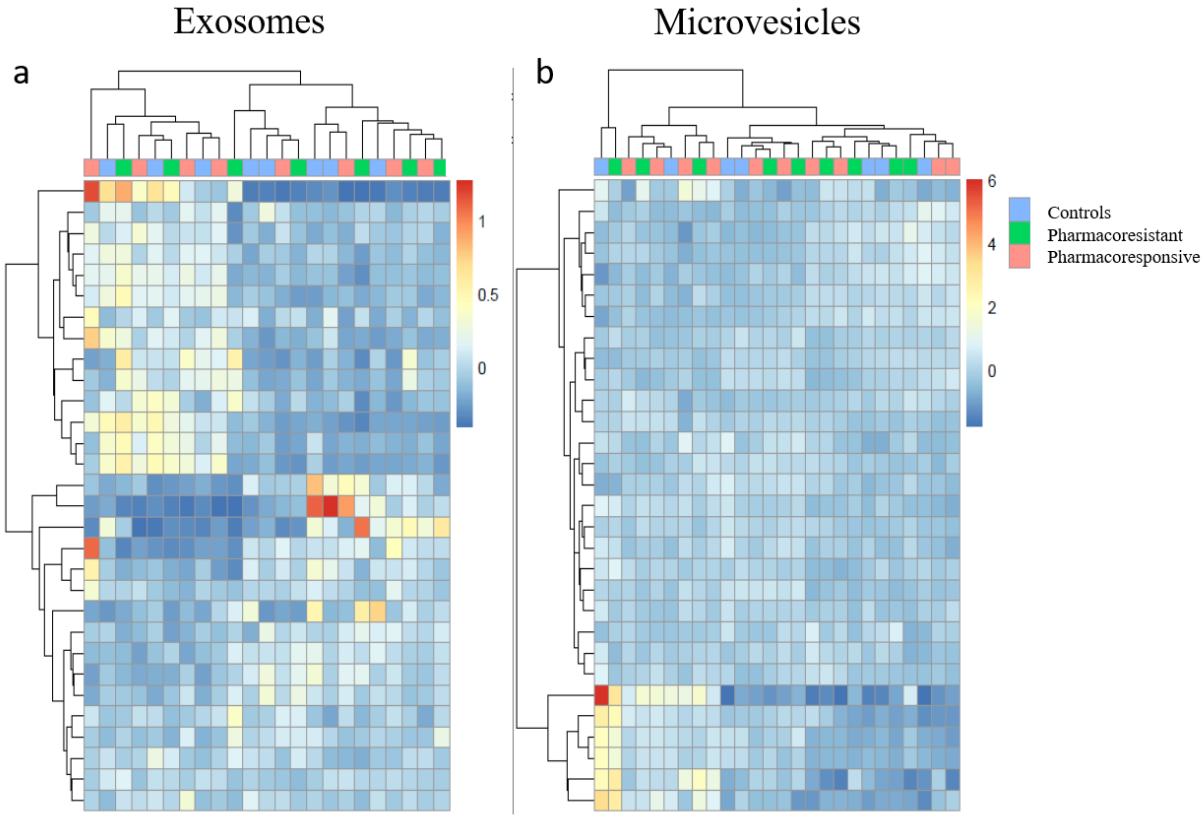

Figure 18. Heat maps showing the differential expression of main de-regulated miRNAs in exosomes (a) and microvesicles (b) across groups of pharmacoresistant patients, pharmacoresponsive patients and controls. Each column represents each subject while each row represents a single de-regulated miRNA. A colour scale represents the level of miRNA expression for each cross. Red represents a higher expression, whereas blue represents a lower expression.

Few miRNAs were found to be significantly de-regulated in their expression in exosomes and microvesicles (Table 10). The analysis was performed first by comparing pharmacoresponsive and pharmacoresistant patients as separate groups with healthy controls, and then by pooling together all patients with epilepsy (Epilepsy Group) against the control group in order to evaluate potential differences related to the underlying disease rather than drug responsiveness. In exosomes, the number of differentially expressed miRNAs was 3 out of 431 in the pharmacoresponsive group, 5 out of 360 in the pharmacoresistant group, and 2 out of 455 in the group of patients with epilepsy. In microvesicles, the differentially expressed miRNAs were 1 out of 387 in the pharmacoresponsive group, 4 out of 365 in the pharmacoresistant group, and 3 out of 475 in the group of patients with epilepsy.

In exosomes, miR-145-5p and miR-3128 were significantly up-regulated and down-regulated, respectively, in patients with epilepsy compared with healthy controls. Five miRNAs were found to be de-regulated in exosomes isolated from pharmacoresistant patients compared with healthy controls. Specifically, miR-145-5p was up-regulated, whereas miR-3128, miR-3150a-3p, miR-3925-5p, and miR-6772-5p were down-regulated in pharmacoresistant patients. In microvesicles, three miRNAs were found to be de-regulated in patients with epilepsy compared with healthy controls: specifically, miR-183-5p was up-regulated, whereas miR-190a-5p, miR-93-3p were down-regulated. Four miRNAs were found to be de-regulated in microvesicles obtained from pharmacoresistant patients compared with healthy controls: these included two up-regulated miRNAs (miR-183-5p, miR-541-3p) and two down-regulated miRNAs (miR-26a-2-3p, miR-190a-5p).

Table 10. Differentially expressed miRNAs extracted from exosomes and microvesicles with the corresponding fold change.

Exosomes			**Microvesicles**		
Pharmacoresponsive patients			**Pharmacoresponsive patients**		
miRNA	**log2 Fold Change**	**Adjusted p-value**	**miRNA**	**log2 Fold Change**	**Adjusted p-value**
hsa-miR-145-5p	22.3826	$7.1x10^{-21}$	**hsa-miR-541-3p**	15.2920	$8.3x10^{-2}$
hsa-miR-3128	-24.1448	$1.6x10^{-9}$			
hsa-miR-3130-5p	-22.3626	$2.1x10^{-7}$			
Pharmacoresistant patients			**Pharmacoresistant patients**		
miRNA	**log2 Fold Change**	**Adjusted p-value**	**miRNA**	**log2 Fold Change**	**Adjusted p-value**
hsa-miR-145-5p	21.4292	$8.0x10^{-18}$	**hsa-miR-183-5p**	4.6549	$1.2x10^{-2}$
hsa-miR-3128	-22.2222	$1.7x10^{-7}$	**hsa-miR-190a-5p**	-5.2128	$5.6x10^{-2}$
hsa-miR-3150a-3p	-20.6969	$9.4x10^{-6}$	**hsa-miR-26a-2-3p**	-21.6580	$4.9x10^{-6}$
hsa-miR-3925-5p	-5.4917	$9.3x10^{-2}$	**hsa-miR-541-3p**	16.1624	$1.5x10^{-2}$
hsa-miR-6772-5p	-21.3577	$1.0x\ 10^{-8}$			
Epilepsy Group			**Epilepsy Group**		
miRNA	**log2 Fold Change**	**Adjusted p-value**	**miRNA**	**log2 Fold Change**	**Adjusted p-value**
hsa-miR-145-5p	22.1490	$2.1\ x10^{-28}$	**hsa-miR-183-5p**	4.0891	$2.5x10^{-2}$
hsa-miR-3128	-24.3720	$1.9x10^{-14}$	**hsa-miR-190a-5p**	-5.0468	$2.3x10^{-2}$
			hsa-miR-93-3p	-3.8941	$4.4x10^{-2}$

Table 11. Validated miRNA-gene-disease ontology interactions in human epilepsy.

	miRNA	**Genes associated**	**Gene description**	**Associated disease terms**
Exosomes	has-miR-3128	SLC6A8	Solute carrier family 6 member 8	Epilepsy, Intractable epilepsy
		WASL	WASP like actin nucleation promoting factor	Epilepsy, Intractable epilepsy
	has-miR3130-5p	L2HGDH	L-2-hydroxyglutarate dehydrogenase	Epilepsy
		GRIN2A	Glutamate ionotropic receptor NMDA type subunit 2A	Epilepsy
		KCTD7	Potassium channel tetramerization domain containing 7	Epilepsy
	has-miR-3150a-3p	ABCC5	ATP binding cassette subfamily C member 5	Epilepsy
	has-miR-145-5p	ABCC1	ATP binding cassette subfamily C member 1	Epilepsy
		ARF6	ADP ribosylation factor 6	Epilepsy
		CYP2C19	Cytochrome P450 family 2 subfamily C member 19	Epilepsy
		EGFR	Epidermal growth factor receptor	Epilepsy, Intractable epilepsy
		FAM3C	Family with sequence similarity 3 member C	Epilepsy, Temporal lobe epilepsy
		MDM2	Mouse double minute 2	Epilepsy, Temporal lobe epilepsy
Microvesicles	has-miR-183-5p	CLN8	Ceroid-lipofuscinosis, neuronal 8	Epilepsy
		RCN2	Reticulocalbin 2	Epilepsy
		RTN4	Reticulon 4	Epilepsy, Temporal lobe epilepsy
		SSTR2	Somatostatin receptor 2	Epilepsy, Temporal lobe epilepsy
	has-miR-190a-5p	KCNMB4	Potassium calcium-activated channel subfamily M regulatory beta subunit 4	Epilepsy
	has-miR-26a-2-3p	GABRG2	Gamma-aminobutyric acid type A receptor gamma2 subunit	Epilepsy

3.2.2.5 miRNA targets and pathway analysis

Significantly differentially expressed miRNAs in pharmacoresistant patients were considered for the pathway analyses. A preliminary analysis was conducted on the mirWalk version 2.0

and 3.0 database (http://zmf.umm.uni-heidelberg.de/apps/zmf/mirwalk2/ and http://mirwalk.umm.uni-heidelberg.de/) in order to predict potential targets of these miRNAs in human epilepsy by using the following keywords: ‘epilepsy’, ‘intractable epilepsy’, and ‘temporal lobe epilepsy’. Seven of the selected miRNAs were found to be related with at least one of these conditions (Table 11).

As a second step, miRWalk was interrogated to investigate pathways associated with validated gene targets for each deregulated miRNAs in pharmacoresistant epilepsy and in the pooled groups of epilepsy patients (Epilepsy Group). This search was performed by selecting “human” as species and “miRBase” as database, and each gene list was pasted in EnrichR to identify potential relevant pathways through “KEGG 2019 pathway”. Only pathways with a p-value<0.05 were considered. Pathway lists were classified into eight categories (cell cycle control, transcription regulation and gene expression, stemness, tissue remodeling ion channel modification and neuronal plasticity, inflammation pathway, apoptosis, cancer and other) to assess up-regulated and down-regulated pathway categories associated with the differentially expressed miRNA identified in extracellular vesicles isolated from pharmacoresistant patients and from the combined epilepsy groups (Figure 19). A limitation of this analysis is that it does not permit to determine the real impact of altered miRNA expression on single genes, or the type(s) of specific alterations in the identified pathways.

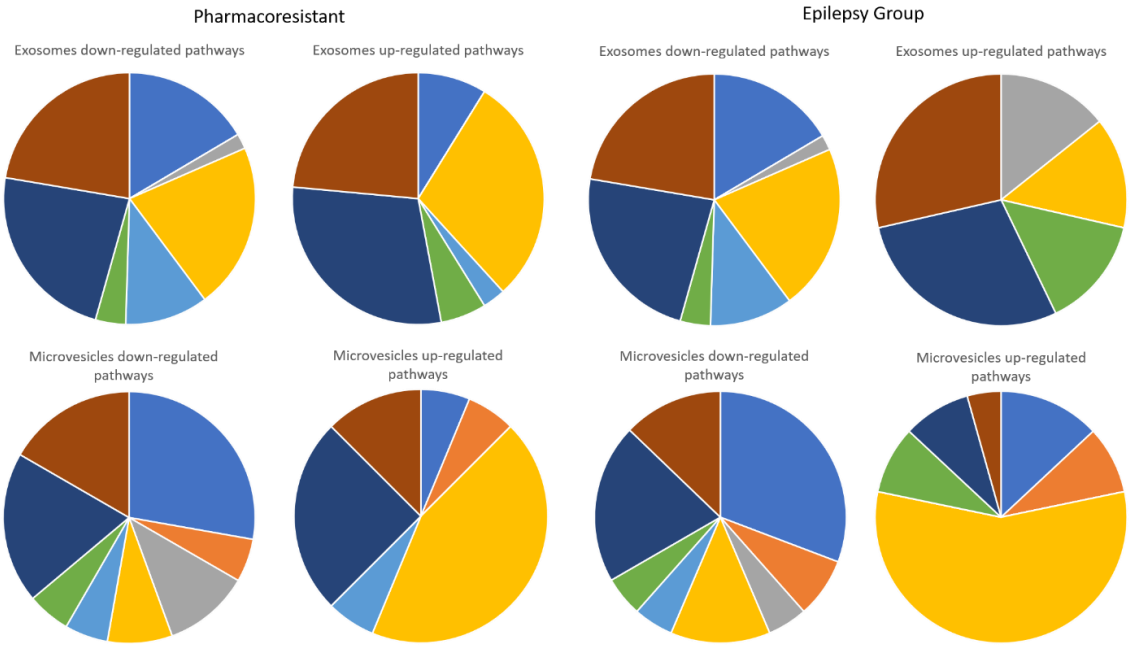

Figure 19. Pie chart of pathway analysis conducted to evaluate the function of down- and up-regulated pathways associated with miRNA differentially expressed (compared with healthy controls) in microvesicles and exosomes isolated from patients with pharmacoresistant epilepsy group and from all patients with epilepsy combined (Epilepsy Group). Pathways were grouped into eight categories (cell cycle control, transcription regulation and gene expression, stemness, tissue remodelling ion channel modification and neuronal plasticity, inflammation pathway, apoptosis, cancer and other). Colour legend: Blue = cell cycle control; orange = transcription regulation and gene expression; grey = stemness; yellow = tissue remodeling ion channel modification and neuronal plasticity; light blue = inflammation pathway; green = apoptosis; dark blue = cancer; brown = other.

4. DISCUSSION AND CONCLUSIONS

4.1 Development and validation of innovative assay methods for new generation AEDs

Many second-generation AEDs have been introduced in the last two decades. Among these, retigabine and perampanel show a novel mechanism of action. In particular retigabine is an activator of potassium channels while perampanel is a non-competitive antagonist of AMPA receptors. Both drugs are characterized by a highly variable pharmacokinetic profile, a potentially high susceptibility to be affected by drug interactions, and a narrow therapeutic index (Patsalos, 2018). To date, the factors that can affect their plasma concentration at steady-state have not been completely characterized, and there is little information on the correlation between their concentration in biological fluids, seizure control and incidence/intensity of adverse effects. Although retigabine was withdrawn from the market by the manufacturer in June 2017 due to its limited utilization following the discovery of cutaneous and retinal side effects, interest in its utilization has been rekindled recently following reports of very promising therapeutic results in children with KCNQ2 encephalopathy, a rare but serious disorder associated with impaired neuronal potassium channel activity. Based on this background, retigabine is currently being evaluated in a Phase III clinical trial aimed at evaluating its efficacy as a precision therapy for KCNQ2 epileptic encephalopathy (Hoffman, 2019).

The elucidation of factors that influence the pharmacokinetics of retigabine and perampanel, and characterization of the correlation between their concentration in body fluids and clinical response, can be relevant to facilitate dose individualization and to improve their efficacy and safety. For retigabine, it would be particularly important to determine whether there is a plasma concentration threshold below which cutaneous and retinal adverse effects are unlikely to occur. Conduction of these studies, however, is dependent on the availability of adequate and convenient assay methods.

Prior to completion of the present work, available assay methods for the determination of retigabine in body fluids were fully adequate for research applications (Deeb et al., 2014; Knebel et al., 2000), but there was no published method that could be conveniently applied to TDM in the routine clinical setting. For perampanel, an HPLC method applicable to TDM had been developed (Franco et al., 2016), but there was scope for improvement particularly with respect to making it applicable to the assay of dried plasma spots, which enhance access to TDM by facilitating storage and shipment of samples.

In the case of retigabine, we developed and validated the first assay method that permits determination of the drug in human plasma by HPLC-UV through a procedure easily applicable to the routine clinical setting. This method offers many advantages compared to those previously published to date (Deeb et al., 2014; Knebel et al., 2000):

- detection is done by UV;
- time consuming evaporation/concentration steps are not needed;
- retigabine and the internal standard are eluted in a small volume of solvent and can be injected directly onto the HPLC system.

The assay uses the combination of an efficient solid-phase extraction, with no need for time-consuming post-extraction evaporation steps, and a monolithic technology that permits to achieve optimal resolution with short chromatographic run times (7 min). Before testing the solid-phase extraction technique, protein precipitation and liquid–liquid extraction were applied and eventually excluded because they led to appearance of numerous peaks from endogenous substances with retention times similar to those of the internal standard and retigabine. An attempt to perform a solid-phase extraction was made initially by using Waters OASIS HLB cartridges, but extracts obtained with these cartridges presented interference from endogenous peaks at the retention time of the internal standard. The selection of EMPORE cartridges for the final assay procedure was associated with minimization of such interference and higher recoveries. The present method shows favourable performance characteristics in terms of accuracy, precision and recovery. No interference is observed with commonly co-prescribed AEDs. Among those tested, only mono-hydroxy-carbazepine (licarbazepine) was found to have a retention time close to that of the internal standard. In samples from patients receiving concomitant treatment with AEDs metabolized to mono-hydroxy-carbazepine (oxcarbazepine or eslicarbazepine acetate), adjustment of chromatographic conditions is required in order to obtain a good separation of mono-hydroxy-carbazepine from the internal standard. In particular, based on additional experiments that we have conducted, replacement of water with potassium hexafluorophosphate 50 mM in the mobile phase is necessary. Other assay performance characteristics are generally satisfactory. In particular, the sensitivity, with a LOQ as low as 25 ng/mL, is adequate to quantitate retigabine concentrations which are generally found in the plasma of patients receiving therapeutic doses of the drug (Ferron et al., 2002).

For perampanel, an HPLC method applicable for TDM purposes has been recently developed (Franco et al, 2016), but there is considerable interest to making it applicable to DPSs, which improve TDM applicability by facilitating storage and shipment of samples. In recent years, use DPSs has attracted increased attention because DPS samples can be collected and stored on paper filters that can be positioned in envelopes and easily stored and shipped. DPS-based assays have been described for antimicrobial agents, antifungals, anti-HIV drugs, and AEDs (Baietto et al 2012; Baietto et al 2013; Baldelli et al 2015; D'Avolio et al 2010; Namdev et al 2018). In particular, Baldelli et al. (2015) described an HPLC method for the determination of ethosuximide, felbamate, lamotrigine, levetiracetam, monohydroxy-carbazepine, rufinamide and zonisamide in DPSs, while more recently D'Urso and collaborators (2019) reported the application of DPSs for the quantitation of nine AEDs using a LC-MS/MS method. In addition, sampling approaches based on dried blood spots have been proposed for the TDM of other AEDs (De Nicolò et al 2017; Shah et al 2013). DPSs are more time consuming compared with dried blood spots, because they require the additional step of plasma separation. However, the advantage of DPS assay results is that they can be directly correlated with those obtained in plasma. Use of dried blood spots can be problematic when drug concentrations differ between plasma and blood cells, because in this case the correlation between blood concentrations and plasma concentrations is influenced by intra- and interindividual differences in hematocrit and drug distribution into blood cells. The method for the determination of perampanel in DPSs, which was developed as part of the work described in the present thesis, is the first such method reported in the literature. The extraction of perampanel from DPSs was optimized testing different solvents, including methanol, acetonitrile, ethyl acetate, and acetic acid. Among those, methanol led to efficient protein precipitation associated to the optimal perampanel extraction. Overlapped glass paper filters spotted with 200 mL of samples and extracted separately (n = 5) were used to investigate the potential sample loss during the spotting phase, and the underlying filter was perampanel-free. The comparison between concentration values measured in plasma and DPS samples collected from patients treated with perampanel showed that the two methods lead to equivalent results, thereby supporting the applicability of DPS-based assays for TDM purposes. The assay sensitivity is adequate for the quantitation of perampanel within the typical therapeutic range (50–1000 ng/mL). Stability data support the benefits of using DPSs for sample storage and shipping. The specificity was not tested for this study as it was previously

evaluated in plasma samples using the same chromatographic conditions irrespective of the matrix analysis (Franco et al., 2016).

4.2 Characterization of miRNAs in extracellular vesicles as potential markers of drug resistance

Several lines of evidence indicate that miRNAs play an important role in modulating epileptogenic processes by regulating neuronal excitability and structure, apoptosis and brain inflammation. In particular, differential expression profiles of numerous miRNAs have been demonstrated in animal models of epileptogenesis after experimentally induced status epilepticus (Bot et al., 2013; Gorter et al., 2014; Kretschmann et al., 2015; Liu et al., 2010) and in studies conducted in experimental and human temporal lobe epilepsy (Aronica et al., 2010; Kan et al., 2012; Omran et al., 2012). Specific miRNAs, such as miR-134, have been found to be overexpressed in patients with active epilepsy (Jimenez-Mateos et al., 2012). Interestingly, silencing miR-134 exerts neuroprotective effects and suppresses seizures after status epilepticus in mice (Jimenez-Mateos et al., 2012), while silencing miR-184 enhances neuronal death in the hippocampus of mice exposed to kainic acid-induced seizures (McKiernan et al., 2012).

Preliminary studies have suggested that the expression of specific miRNAs may be altered in patients with drug-resistant epilepsy (Wang et al 2015 a,b). In an initial study, Wang et al. (2015a) investigated miRNA profiles in plasma of 147 patients with epilepsy and 142 healthy controls. Six miRNAs were found to be de-regulated: four of them (Let-7d-5p, miR-106b-5p, miR-130a-3p, and miR-146a-5p) were significantly increased and two (miR-15a-5p and miR-194-5p) were significantly down-regulated compared to healthy controls. In particular, the study suggested that miR-106b-5p, a member of miRNA family implicated in cell proliferation, may provide a diagnostic biomarker for epilepsy with sensitivity and specificity of 81% and 80% respectively (Wang et al., 2015a). In a second study conducted by the same authors, miRNAs expression levels were evaluated in 77 patients with drug-resistant epilepsy, 81 patients with drug-responsive epilepsy and 85 healthy controls. Differences in the expression profile of circulating miRNAs between the drug-resistant group and the drug-responsive group were found. In particular, a significant de-regulation of miR-194-5p, miR-301a-3p, miR30b-5p, miR342-5p and miR4446-3p in the drug-resistant group compared with both the drug-responsive group and the control group was reported. Among these miRNAs, miR-301a-3p was

associated with a diagnosis of pharmacoresistant epilepsy with a sensitivity and a specificity of 80.5% and 81.2%, respectively. The same miRNA was also inversely correlated with seizure severity (Wang et al., 2015b). Although these results were interesting, the differences between pharmacoresistant and pharmacoresponsive patients were not of sufficient magnitude to permit a reliable discrimination between these populations. Moreover, confirmation of these findings in better characterized patient populations is needed.

Another recent study explored the expression level of miRNAs isolated from exosomes in patients with mesial temporal lobe epilepsy associated with hippocampal sclerosis (Yan et al., 2017). In that study, two miRNAs were found to be up-regulated and 48 were founs to be down-regulated in the temporal lobe epilepsy patients compared with healthy controls. Among them, six miRNAs (miR-3613-5p, miR-4668-5p, miR-8071, miR-197-5p, miR-4322, and miR-6781-5p) were significantly differentially expressed and underwent validation in further studies. The authors concluded that among the six candidate miRNAs, miR-8071 had the best diagnostic value for mesial temporal lobe epilepsy with hippocampal sclerosis, with 83.33% sensitivity and 96.67% specificity (Yan et al., 2017). To date, however, there have been no formal studies of miRNA expression in extracellular vesicles from patients with pharmacoresistant epilepsy. This is an important knowledge gap, because extracellular vesicles represent the main miRNAs transport vehicles, and are highly enriched in miRNA compared with whole serum.

Our findings extend these observations by providing additional evidence that certain miRNAs can be de-regulated in patients with epilepsy, and that differences in miRNA expression may exist between patients with drug refractory and patients with drug responsive focal epilepsy. Closer evaluation of results, on the other hand, reveals that none of the miRNAs that had been reported to be de-regulated in the studies mentioned above was differentially expressed in our patients. However, when we compare our results with those obtained in the only study that investigated miRNAs expression in exosomes isolated from plasma samples collected from patients with focal epilepsy (Yan et al., 2017), we can identify a non-statistically significant signal for 9 (18%) of the 50 miRNAs found to be de-regulated by Yan et al (2017) to be also de-regulated in the group of our epilepsy patients: these include hsa-miR-1307-3p, hsa-miR-150-3p, hsa-miR-3180-3p, hsa-miR-4689, hsa-miR-4721, hsa-miR-483-5p, hsa-miR-6124, hsa-miR-671-5p, hsa-miR-8071. The partial discrepancies between our findings and those reported by Yan et al. (2017) could be explained by limitations in sample size, differences in

the characteristics of the patients included in the two studies, and technical issues related to the assay methodology used.

While the limitations in the interpretation of these findings are acknowledged, overall the currently available evidence does allow to conclude that expression of individual miRNAs in exosomes and microvesicles isolated from plasma does not permit to differentiate between pharmacoresistant and pharmacoresponsive focal epilepsy patients with a level of accuracy sufficient to guide clinical management. Admittedly, such differentiation might be possible by investigating the discriminatory power of specific miRNA combination profiles rather than individual miRNAs, but evaluation of complex profiles will require costly and time-consuming exploratory and confirmatory studies in large populations of patients. With advances in technology, and reduction in the cost of assay methods, these studies could become more readily feasible in the future. Results of these studies could also be of value in elucidating specific mechanisms of epileptogenesis and pharmacoresistance, which in turn could lead to rational development of more effective therapies. In our own study, interrogation of libraries did allow to identify potential relationships between identified de-regulated miRNAs and a number of genes/pathways known to be relevant for epileptogenesis and for drug resistance. Elaboration on the specific roles of these pathways in explaining diffrences in drug responsiveness in our population remains open to speculation. The elucidation of these roles will be dependent on the acquisition of futher information, including results of confirmatory studies in larger populations of patients.

5. REFERENCES

1. Aronica E, Fluiter K, Iyer A, Zurolo E, Vreijling J, van Vliet EA, Baayen JC, Gorter JA. Expression pattern of miR-146a, an inflammation-associated microRNA, in experimental and human temporal lobe epilepsy. Eur J Neurosci. 2010;31:1100-7.

2. Baietto L, D'Avolio A, Ariaudo A, Corcione S, Simiele M, Cusato J, Urbino R, Di Perri G, Ranieri VM, De Rosa FG. Development and validation of a new UPLC-PDA method to quantify linezolid in plasma and in dried plasma spots. J Chromatogr B Analyt Technol Biomed Life Sci. 2013;936:42-7.

3. Baietto L, D'Avolio A, Marra C, Simiele M, Cusato J, Pace S, Ariaudo A, De Rosa FG, Di Perri G. Development and validation of a new method to simultaneously quantify triazoles in plasma spotted on dry sample spot devices and analysed by HPLC-MS. J Antimicrob Chemother. 2012;67:2645-9

4. Baldelli S, Cattaneo D, Giodini L, Baietto L, Di Perri G, D'Avolio A, Clementi E. Development and validation of a HPLC-UV method for the quantification of antiepileptic drugs in dried plasma spots. Clin Chem Lab Med. 2015;53:435-44.

5. Basic S, Hajnsek S, Bozina N, Filipcic I, Sporis D, Mislov D, Posavec A. The influence of C3435T polymorphism of ABCB1 gene on penetration of phenobarbital across blood–brain barrier in patients with generalized epilepsy. Seizure Eur J Epilepsy. 2008;17:524-530.

6. Bot AM, Dębski KJ, Lukasiuk K. Alterations in miRNA levels in the dentate gyrus in epileptic rats. PLoS One. 2013;8:e76051.

7. Choy M, Dubé CM, Patterson K, Barnes SR, Maras P, Blood AB, Hasso AN, Obenaus A, Baram TZ. A novel, noninvasive, predictive epilepsy biomarker with clinical potential. J Neurosci 2014; 34:8672–8684.

8. Cohen AS, Lin DD, Quirk GL, Coulter DA. Dentate granule cell GABA(A) receptors in epileptic hippocampus: enhanced synaptic efficacy and altered pharmacology. Eur J Neurosci 2003;17:1607-1616

9. Danhof M, Alvan G, Dahl SG, Kuhlmann J, Paintaud G. Mechanism-based pharmacokinetic-pharmacodynamic modeling-a new classification of biomarkers. Pharm Res. 2005;22:1432-7.

10. D'Avolio A, Simiele M, Siccardi M, Baietto L, Sciandra M, Bonora S, Di Perri G. HPLC-MS method for the quantification of nine anti-HIV drugs from dry plasma spot on glass filter and their long term stability in different conditions. J Pharm Biomed Anal. 2010;52:774-80.

11. Deeb S, McKeown DA, Torrance HJ, Wylie FM, Logan BK, Scott KS. Simultaneous analysis of 22 antiepileptic drugs in postmortem blood, serum and plasma using LC-MS-MS with a focus on their role in forensic cases. J Anal Toxicol. 2014;38:485-94.

12. De Nicolò A, Cantù M, D'Avolio A. Matrix effect management in liquid chromatography mass spectrometry: the internal standard normalized matrix effect. Bioanalysis. 2017;9:1093-1105.

13. Depondt C, Shorvon SD. Genetic association studies in epilepsy pharmacogenomics: lessons learnt and potential applications. Pharmacogenomics. 2006;7:731-45.

14. Devinsky O, Vezzani A, O'Brien TJ, Jette N, Scheffer IE, de Curtis M, Perucca P. Epilepsy. Nat Rev Dis Primers. 2018;4:18024.

15. D'Urso A, Rudge J, Patsalos PN, de Grazia U. Volumetric absorptive microsampling: A new sampling tool for therapeutic drug monitoring of anti-epileptic drugs. Ther Drug Monit. 2019 May 27.

16. Engel J Jr, Pitkänen A, Loeb JA, Dudek FE, Bertram EH 3rd, Cole AJ, Moshé SL, Wiebe S, Jensen FE, Mody I, Nehlig A, Vezzani A. Epilepsy biomarkers. Epilepsia. 2013;54Suppl4:61-9.

17. European Medicines Agency. EMA/CHMP/EWP, Committee for Medicinal Products for Human Use: Guideline on Bioanalytical Method Validation, 2011. Available at: http://www.ema.europa.eu/docs/en_GB/document_library/Scientific_guideline/2011/08/WC500109686.pdf

18. Fang M, Xi ZQ, Wu Y, Wang XF. A new hypothesis of drug refractory epilepsy: neural network hypothesis. Med Hypotheses. 2011;76:871-6.

19. Ferrie CD. Preventing misdiagnosis of epilepsy. Arch Dis Child. 2006;91:206-209.

20. Ferron GM, Paul J, Fruncillo R, Richards L, Knebel N, Getsy J, Troy S. Multiple-dose, linear, dose-proportional pharmacokinetics of retigabine in healthy volunteers. J. Clin. Pharmacol. 2002;42:175-182.

21. Fisher RS, Acevedo C, Arzimanoglou A, Bogacz A, Cross JH, Elger CE, Engel J Jr, Forsgren L, French JA, Glynn M, Hesdorffer DC, Lee BI, Mathern GW, Moshé SL, Perucca E, Scheffer IE, Tomson T, Watanabe M, Wiebe S. ILAE official report: a practical clinical definition of epilepsy. Epilepsia. 2014;55:475-82.

22. Fisher RS, Cross JH, French JA, Higurashi N, Hirsch E, Jansen FE, Lagae L, Moshé SL, Peltola J, Roulet Perez E, Scheffer IE, Zuberi SM. Operational classification of seizure types by the international league against epilepsy: position paper of the ILAE commission for classification and terminology. Epilepsia. 2017;58:522–530.

23. Fisher RS, van Emde Boas W, Blume W, Elger C, Genton P, Lee P, Engel J Jr. Epileptic seizures and epilepsy: definitions proposed by the International League Against Epilepsy (ILAE) and the International Bureau for Epilepsy (IBE). Epilepsia. 2005;46:470-2.

24. Franco V, Marchiselli R, Fattore C, Tartara E, De Sarro G, Russo E, Perucca E. Development and Validation of an HPLC-UV Assay for the Therapeutic Monitoring of the New Antiepileptic Drug Perampanel in Human Plasma. Ther Drug Monit. 2016;38:744-750.

25. Fromm MF. Importance of P-glycoprotein at blood–tissue barriers. Trends Pharmacol Sci 2004;25:423-429.

26. Galanopoulou AS, Moshé SL. In search of epilepsy biomarkers in the immature brain: goals, challenges and strategies. Biomark Med. 2011;5:615-28.

27. Gastaut, H. Classification of the epilepsies. Proposal for an international classification. Epilepsia. 1969;10: 14-21.

28. Gastaut, H. Clinical and electroencephalographic classification of epileptic seizures. Epilepsia. 1970;11:102.

29. Gorter JA, Iyer A, White I, Colzi A, van Vliet EA, Sisodiya S, Aronica E. Hippocampal subregion-specific microRNA expression during epileptogenesis in experimental temporal lobe epilepsy. Neurobiol Dis. 2014;62:508-20.

30. Hoffman M. XEN496 being developed for KCNQ2 epileptic encephalopathy. https://www.neurologylive.com/clinical-focus/xen496-kcnq2-epileptic-encephalopathy-being-developed (accessed September 6, 2019)

31. ILAE 1981ILAE; Commission of Classification and Terminology of the International League Against Epilepsy: proposal for revised clinical and electroencephalographic classification of epileptic seizures. Epilepsia. 1981;22:489–501.

32. ILAE; Commission on Classification and Terminology of the International League Against Epilepsy: proposal for revised classification of epilepsies and epileptic syndromes. Epilepsia. 1989;30:389–399.

33. Immonen R, Kharatishvili I, Gröhn O, Pitkänen A. MRI biomarkers for post-traumatic epileptogenesis. J Neurotrauma 2013;30:1305–1309.

34. Jimenez-Mateos EM, Engel T, Merino-Serrais P, McKiernan RC, Tanaka K, Mouri G, Sano T, O'Tuathaigh C, Waddington JL, Prenter S, Delanty N, Farrell MA, O'Brien DF, Conroy RM, Stallings RL, DeFelipe J, Henshall DC. Silencing microRNA-134 produces neuroprotective and prolonged seizure-suppressive effects. Nat Med. 2012;18:1087-94

35. Kan AA, van Erp S, Derijck AA, de Wit M, Hessel EV, O'Duibhir E, de Jager W, Van Rijen PC, Gosselaar PH, de Graan PN, Pasterkamp RJ. Genome-wide microRNA profiling of human temporal lobe epilepsy identifies modulators of the immune response. Cell Mol Life Sci. 2012;69:3127-45.

36. Katz R. Biomarkers and surrogate markers: an FDA perspective. NeuroRx. 2004;1:189-95.

37. Knebel NG, Grieb S, Leisenheimer S, Locher M. Determination of retigabine and its acetyl metabolite in biological matrices by on-line solid-phase extraction (column switching) liquid chromatography with tandem mass spectrometry, J. Chromatogr. B Biomed. Sci. Appl. 2000;748:97-111.

38. Kolanowska M, Kubiak A, Jażdżewski K, Wójcicka A. MicroRNA Analysis Using Next-Generation Sequencing. Methods Mol Biol. 2018;1823:87-101.

39. Kretschmann A, Danis B, Andonovic L, Abnaof K, van Rikxoort M, Siegel F, Mazzuferi M, Godard P, Hanon E, Fröhlich H, Kaminski RM, Foerch P, Pfeifer A.

Different microRNA profiles in chronic epilepsy versus acute seizure mouse models. J Mol Neurosci. 2015;55:466-79.

40. Kumar A, Chugani HT. Delineating cortical networks underlying epileptic encephalopathy and cognitive impairment with PET: a perspective. J Nucl Med. 2011;52:8-9.
41. Kwan P, Arzimanoglou A, Berg AT, Brodie MJ, Allen Hauser W, Mathern G, Moshé SL, Perucca E, Wiebe S, French J. Definition of drug resistant epilepsy: consensus proposal by the ad hoc Task Force of the ILAE Commission on Therapeutic Strategies. Epilepsia. 2010;51:1069-77.
42. Kwan, P, Brodie MP. Potential Role of Drug Transporters in the Pathogenesis of Medically Intractable Epilepsy. Epilepsia. 2005;46:224-235.
43. Kwon CS, Liu M, Quan H, Wiebe S, McChesney J, Wirrell E, Hamiwka L, Jetté N. The incidence of injuries in persons with and without epilepsy—a population-based study. Epilepsia. 2010;51:2247-53.
44. Liu DZ, Tian Y, Ander BP, Xu H, Stamova BS, Zhan X, Turner RJ, Jickling G, Sharp FR. Brain and blood microRNA expression profiling of ischemic stroke, intracerebral hemorrhage, and kainate seizures. J Cereb Blood Flow Metab. 2010;30:92-101.
45. Loeb JA. A human systems biology approach to discover new drug targets in epilepsy. Epilepsia. 2010;51Suppl3:171-7.
46. Löscher W, Klitgaard H, Twyman RE, Schmidt D. New avenues for anti-epileptic drug discovery and development. Nat Rev Drug Discov. 2013;12:757-76.
47. Loup F, Wieser HG, Yonekawa Y, Aguzzi A, Fritschy JM. Selective alterations in GABAA receptor subtypes in human temporal lobe epilepsy. J Neurosci 2000;20:5401-5419.
48. Love MI, Huber W, Anders S. Moderated estimation of fold change and dispersion for RNA-seq data with DESeq2. Genome Biol. 2014;15:550.
49. Mardis ER. Next-generation sequencing platforms. Annu Rev Anal Chem (Palo Alto Calif). 2013;6:287-303.

50. McKiernan RC, Jimenez-Mateos EM, Sano T, Bray I, Stallings RL, Simon RP, Henshall DC. Expression profiling the microRNA response to epileptic preconditioning identifies miR-184 as a modulator of seizure-induced neuronal death. Exp Neurol. 2012;237:346-54.

51. McNamara JO. Emerging insights into the genesis of epilepsy. Nature. 1999 24;399:A15-22.

52. Middlebrooks EH, Ver Hoef L, Szaflarski JP. Neuroimaging in Epilepsy. Curr Neurol Neurosci Rep. 2017;17:32.

53. Moshé SL, Perucca E, Ryvlin P, & Tomson T. Epilepsy: new advances. The Lancet. 2015;385:884-898.

54. Namdev KK, Dwivedi J, Chilkoti DC, Sharma S. A simple, rapid and stability indicating validated method for quantification of lamotrigine in human plasma and dry plasma spot using LC-ESI-MS/MS: Application in clinical study. J Chromatogr B Analyt Technol Biomed Life Sci. 2018;1072:362-369.

55. Ngugi AK, Kariuki SM, Bottomley C, Kleinschmidt I, Sander JW, Newton CR. Incidence of epilepsy: A systematic review and meta-analysis. Neurology. 2011;77:1005-1012.

56. Omran A, Peng J, Zhang C, Xiang QL, Xue J, Gan N, Kong H, Yin F. Interleukin-1β and microRNA-146a in an immature rat model and children with mesial temporal lobe epilepsy. Epilepsia. 2012;53:1215-24.

57. Patsalos PN, Spencer EP, Berry DJ. Therapeutic Drug Monitoring of Antiepileptic Drugs in Epilepsy: A 2018 Update. Ther Drug Monit. 2018;40:526-548.

58. Perucca E. Overtreatment in epilepsy: adverse consequences and mechanisms. Epilepsy Res. 2002;52:25-33.

59. Perucca E, Kwan P. Overtreatment in epilepsy: how it occurs and how it can be avoided. CNS Drugs. 2005;19:897-908.

60. Perucca E, Tomson T. The pharmacological treatment of epilepsy in adults. Lancet Neurol. 2011;10:446-56.

61. Pitkänen A, Löscher W, Vezzani A, Becker AJ, Simonato M, Lukasiuk K, Gröhn O, Bankstahl JP, Friedman A, Aronica E, Gorter JA, Ravizza T, Sisodiya SM, Kokaia M, Beck H. Advances in the development of biomarkers for epilepsy. Lancet Neurol. 2016;15:843-856.

62. Pitkänen A, Lukasiuk K. Mechanisms of epileptogenesis and potential treatment targets. Lancet Neurol. 2011;10:173-86.

63. Raoof R, Jimenez-Mateos EM, Bauer S, Tackenberg B, Rosenow F, Lang J, Onugoren MD, Hamer H, Huchtemann T, Körtvélyessy P, Connolly NMC, Pfeiffer S, Prehn JHM, Farrell MA, O'Brien DF, Henshall DC, Mooney C. Cerebrospinal fluid microRNAs are potential biomarkers of temporal lobe epilepsy and status epilepticus. Sci Rep. 2017;7:3328.

64. Raspall-Chaure M, Neville BG, Scott RC. The medical management of the epilepsies in children: conceptual and practical considerations. Lancet Neurol. 2008;7:57-69.

65. Regesta G, Tanganelli P. Clinical aspects and biological bases ofdrug-resistant epilepsies. Epilepsy Res. 1999;34:109-22.

66. Remy SS, Gabriel B, Urban D, Dietrich T, Lehmann C, Elger U, Heinemann H. Beck. A novel mechanism underlying drug resistance in chronic epilepsy. Ann Neurol. 2003;53:469-79.

67. Rogawski MA. The intrinsic severity hypothesis of pharmacoresistance to antiepileptic drugs. Epilepsia. 2013;54 Suppl 2:33-40.

68. Shah NM, Hawwa AF, Millership JS, et al. A simple bioanalytical method for the quantification of antiepileptic drugs in dried blood spots. *J Chromatogr B Analyt Technol Biomed Life Sci.* 2013;923:65-73.

69. Scheffer IE, Berkovic S, Capovilla G, Connolly MB, French J, Guilhoto L, Hirsch E, Jain A, Mathern GW, Moshé SL, Nordli DR, Perucca E, Tomson T, Wiebe S, Zhang Y, Zuberi SM. ILAE classification of the epilepsies: position paper of the ILAE Commission for Classification and Terminology. Epilepsia 2017;58:512–521.

70. Schinkel AH, Jonker JW. Mammalian drug efflux transporters of the ATP binding cassette (ABC) family: an overview. Adv Drug Deliv Rev 2003;55:3-29

71. Schmidt D, Löscher W. Drug resistance in epilepsy: putative neurobiologic and clinical mechanisms.Epilepsia. 2005;46:858-77.

72. Siddiqui A, Kerb R, Weale ME, Brinkmann U, Smith A, Goldstein DB, Wood NW, Sisodiya SM. Association of multidrug resistance in epilepsy with a polymorphism in the drug-transporter gene ABCB1. N Engl J Med. 2003;348:1442-1448.

73. Sueri C, Gasparini S, Balestrini S, Labate A, Gambardella A, Russo E, Leo A, Casarotto S, Pittau F, Trimboli M, Cianci V, Ascoli M, Cavalli SM, Ferrigno G, Aguglia U, Ferlazzo E. Diagnostic Biomarkers of Epilepsy. Curr Pharm Biotechnol. 2018;19:440-450.

74. Théry C, Witwer KW, Aikawa E, Alcaraz MJ, Anderson JD, Minimal information for studies of extracellular vesicles 2018 (MISEV2018): a position statement of the International Society for Extracellular Vesicles and update of the MISEV2014 guidelines. J Extracell Vesicles. 2018;7:1535750.

75. Timmerman P, White S, Cobb Z, de Vries R, Thomas E, van Baar B; European Bioanalysis Forum. Update of the EBF recommendation for the use of DBS in regulated bioanalysis integrating the conclusions from the EBF DBS-microsampling consortium. Bioanalysis. 2013;5:2129-36.

76. Timmerman P, White S, Globig S, Lüdtke S, Brunet L, Smeraglia J. EBF recommendation on the validation of bioanalytical methods for dried blood spots. Bioanalysis. 2011;3:1567-75.

77. Tishler, D., K. Weinberg, D. Hinton, N. Barbaro, G. Annett and R. C. MDR1 gene expression in brain of patients with medically intractable epilepsy. Epilepsia. 1995;36:1-6.

78. Volk HA, Arabadzisz D, Fritschy JM, Brandt C, Bethman K, Löscher W. Antiepileptic drug resistant rats differ from drug responsive rats in hippocampal neurodegeneration and GABAA-receptor ligand-binding in a model of temporal lobe epilepsy. Neurobiol Dis 2006;21:633-646.

79. Vreugdenhil M, van Veelen CW, van Rijen PC, Lopes da Silva FH, Wadman WJ. Effect of valproic acid on sodium currents in cortical neurons from patients with pharmaco-resistant temporal lobe epilepsy. Epilepsy Res. 1998;32:309-20.

80. Walker MC, Sander JW. Difficulties in extrapolating from clinical trial datato clinical practice: the case of antiepileptic drugs. Neurology. 1997;49:333-7.

81. Wang J, Yu JT, Tan L, Tian Y, Ma J, Tan CC, Wang HF, Liu Y, Tan MS, Jiang T, Tan L. Genome-wide circulating microRNA expression profiling indicates biomarkers for epilepsy. Sci Rep. 2015a;5:9522.

82. Wang J, Tan L, Tan L, Tian Y, Ma J, Tan CC, Wang HF, Liu Y, Tan MS, Jiang T, Yu JT. Circulating microRNAs are promising novel biomarkers for drug-resistant epilepsy. Sci Rep. 2015b;5:10201.

83. Wirrell EC. Predicting pharmacoresistance in pediatric epilepsy. Epilepsia. 2013;54 Suppl 2:19-22.

84. Yan S, Zhang H, Xie W, Meng F, Zhang K, Jiang Y, Zhang X, Zhang J. Altered microRNA profiles in plasma exosomes from mesial temporal lobe epilepsy with hippocampal sclerosis. Oncotarget. 2017;8:4136-4146.

85. Younus I, Reddy DS. Epigenetic interventions for epileptogenesis: A new frontier for curing epilepsy. Pharmacol Ther. 2017;177:108-122.